


8-2023

UTILIZING CRISPR CAS9 TO VISUALIZE DOPAMINE RECEPTORS IN CAENORHABDITIS ELEGANS

Lauren Michelle Velasquez
California State University – San Bernardino

Follow this and additional works at: <https://scholarworks.lib.csusb.edu/etd>

 Part of the [Genetics Commons](#), [Laboratory and Basic Science Research Commons](#), [Molecular and Cellular Neuroscience Commons](#), and the [Molecular Biology Commons](#)

Recommended Citation

Velasquez, Lauren Michelle, "UTILIZING CRISPR CAS9 TO VISUALIZE DOPAMINE RECEPTORS IN CAENORHABDITIS ELEGANS" (2023). *Electronic Theses, Projects, and Dissertations*. 1774.
<https://scholarworks.lib.csusb.edu/etd/1774>

This Thesis is brought to you for free and open access by the Office of Graduate Studies at CSUSB ScholarWorks. It has been accepted for inclusion in Electronic Theses, Projects, and Dissertations by an authorized administrator of CSUSB ScholarWorks. For more information, please contact scholarworks@csusb.edu.

UTILIZING CRISPR CAS9 TO VISUALIZE DOPAMINE RECEPTORS IN
CAENORHABDITIS ELEGANS

A Thesis
Presented to the
Faculty of
California State University,
San Bernardino

In Partial Fulfillment
of the Requirements for the Degree
Master of Science
in
Biology

by
Lauren Michelle Velasquez
August 2023

UTILIZING CRISPR CAS9 TO VISUALIZE DOPAMINE RECEPTORS IN
CAENORHABDITIS ELEGANS

A Thesis
Presented to the
Faculty of
California State University,
San Bernardino

by
Lauren Michelle Velasquez

August 2023

Approved by:

Michael Chao, Committee Chair, Biology

Laura Newcomb, Committee Member

Daniel Nickerson, Committee Member

© 2023 Lauren Michelle Velasquez

ABSTRACT

Dopamine (DA) is a neurotransmitter with imperative implications in many functions including movement, reward, and cognition. Studying the pathways of dopaminergic neurons at multiple levels allows us to understand the ways in which these systems can go wrong. We study dopamine in a model system such as the worm *Caenorhabditis elegans* because of its relatively simple and well-characterized nervous system. DA is involved in regulating chemosensory behaviors in worms. The purpose of this research project is to definitively answer the following question: Are the dopamine receptors DOP-1 and DOP-4 expressed in chemosensory neurons? Previous reporter assays show that neither of these receptors are located in these neurons of interest, although behavioral assays involving knockouts of the genes encoding these receptors show behavioral deficits. Classic transgenic techniques, such as those used originally to visualize the locations of dopamine receptors, involved injecting exogenous plasmid DNA containing promoter-reporter gene fusions into worm gonads to be expressed in offspring. However, these reporter constructs may exhibit different expression patterns than endogenous genes. By using CRISPR/Cas9 to target the *dop-1* gene encoding the DOP-1 receptor, the coding sequence for a reporter gene was inserted to visualize where exactly this gene is expressed in its native chromosomal context, with specific attention to neurons involved in chemosensory behavior. While we were able to insert our reporter at

the *dop-1* locus, fluorescence was not detected. Future work may build on our constructs to examine where this gene is being expressed.

ACKNOWLEDGEMENTS

Dr. Michael Chao

Dr. Laura Newcomb

Dr. Daniel Nickerson

CSUSB College of Natural Sciences, Biology department

Chao Lab students:

Cory Kunkel

Jolene Jensen

CSUSB Office of Student Research

DEDICATION

For Vincent.

TABLE OF CONTENTS

ABSTRACT	iii
ACKNOWLEDGEMENTS.....	v
CHAPTER ONE: INTRODUCTION	1
Dopamine is an Important Neurotransmitter	1
<i>dop-1::gfp</i> and <i>dop-4::gfp</i> Expression in Head Neurons	5
Classic Gene Editing Techniques in <i>Caenorhabditis elegans</i>	7
CRISPR/Cas9 as a Precision Gene Editing Tool.....	8
CHAPTER TWO: MATERIALS AND METHODS	10
Strategy 1: Oligonucleotide Based Approach	10
CRISPR Sequence Design	10
Plasmids	10
PCR	10
Strains and Culture	11
Microinjection	12
Screening for Edits.....	12
Worm Lysis	13
Strategy 2: Plasmid-Based Approach	13
Plasmids	13
Recombinant DNA / Plasmid Constructs.....	13
Sequencing	14
Strains and Culture	14
Worm Lysis	15

Microinjection	15
Selection Strategy	15
Self-Excising Cassette Removal	16
CHAPTER THREE: RESULTS.....	17
Strategy Overview	17
Strategy 1: Oligonucleotide Based Approach	18
Strategy 2: Plasmid Based Approach	20
CHAPTER FOUR: DISCUSSION	24
APPENDIX A: FIGURES	33
APPENDIX B: TABLES	53
APPENDIX C: LIST OF ABBREVIATIONS	60
REFERENCES	62

CHAPTER ONE:

INTRODUCTION

Dopamine is an Important Neurotransmitter

Dopamine (DA) is a neurotransmitter with many important functions including movement (Cousins & Salamone, 1996), reward (Koob, 1992), learning and memory (Le Moal & Simon, 1991), cognition, and hormone release (Saiardi et al., 1997). Studying the pathways of dopaminergic neurons at multiple levels allows us to understand the ways in which these systems can go wrong in pathologies such as Parkinson's disease (Gerfen, 1992; Lang AE & Lozano AM, 1998), addiction (Koob & Bloom, 1988), schizophrenia (Knable & Weinberger, 1997), or pituitary tumors (Saiardi et al., 1997). Interestingly, dopamine assists in other functions as well, including interspecies interactions, indicating a conserved role across taxa (Vidal-Gadea & Pierce-Shimomura, 2012).

We study dopamine in a model system, the nematode *Caenorhabditis elegans*, because of its relatively simple and well-characterized nervous system. *C. elegans* have 302 neurons and their connectivity is known down to the synapse level (Durbin, 1987; Varshney et al., 2011; White et al., 1986). We are interested in understanding the molecular and cellular mechanisms that underlie DA regulation of behavior. One aspect of understanding these mechanisms is identifying the molecular components of the DA signaling pathways and elucidating in which neurons these components are expressed. Our specific goal for this project is to determine if *C. elegans* DA receptors are expressed in

neurons that are known to be involved in chemosensory behaviors, and more specifically, the amphid sensory ASH neuron and connecting interneurons (Bargmann, 1998; Hilliard et al., 2002, 2004; Kaplan & Horvitz, 1993; Sambongi et al., 1999).

There are eight dopamine producing neurons in the *C. elegans* hermaphrodite, with an additional six in the tails of the male (Sulston et al., 1975). These neurons are identified through expression of the *cat-2* gene, which codes for tyrosine hydroxylase (Lints & Emmons, 1999), a necessary component for dopamine biosynthesis. Dopamine is synthesized from the amino acid tyrosine in a two-step sequence. Tyrosine is modified by the enzyme tyrosine hydroxylase to the intermediate levadopa (L-DOPA), then L-DOPA is converted by dopa-decarboxylase to dopamine. In *C. elegans*, dopamine signaling is transduced both classically, through synapses, as well as extrasynaptically, such that neurons containing dopamine receptors need not be directly post-synaptic to dopamine producing neurons (Chase et al., 2004). The *C. elegans* genome codes for four putative DA receptors, DOP-1 through DOP-4, of the seven transmembrane G protein-coupled receptor family (Chase et al., 2004; Missale et al., 1998; Sanyal et al., 2004; Sugiura et al., 2005; Suo et al., 2002, 2003; Tsalik et al., 2003).

Of these four, previous research suggests that the DOP-1 and DOP-4 DA receptors may function in neurons of the chemosensory avoidance behavioral circuit involving the ASH sensory neurons and connecting interneurons.

Chemosensory neurons are bilaterally symmetrical, such that there are the ASHL and ASHR, collectively referred to as the ASH neuron (White et al., 1986). The ASH neuron is a polymodal sensory neuron that functions in the chemosensory avoidance pathway in response to noxious stimuli such as octanol, SDS, quinine, copper, cadmium and hydrogen ions (Bargmann, 1998; Hilliard et al., 2004; Sambongi et al., 1999). In response to aversive stimuli, *C. elegans* avoidance behavior is characterized by reversing and changing direction of movement (Culotti & Russell, 1978), a response generated by prolonged activation of the ASH neuron (Faumont & Lockery, 2006; Zengcai V Guo et al., 2009). The ASH neuron connects with the command interneurons, AVA, AVB, and AVD, which navigate forward and reverse locomotion (White et al., 1986) (

Figure 1). These command neurons integrate input and communicate with the motor neurons, DA, VA, DB, and VB, which then enact the appropriate behavior.

In *C. elegans*, dopamine modulates many behavioral responses to guide the animal's behavior. Ezcurra et al. (2011) found that dopamine modulates ASH responses to aversive stimuli while in the presence of food. When off their food substrate, *C. elegans* initiate more reversals in response to noxious stimuli such as copper and glycerol than while in the presence of food. The presence of food sensed by dopaminergic neurons elicits enhanced neuronal responses within the ASH neuron to these chemical repellants (Ezcurra et al., 2011). Animals containing the mutant *cat-2(e1112)* allele defective for tyrosine hydroxylase, and

thus defective in dopamine biosynthesis, have longer latency to reversal when on food. However, exogenous dopamine rescued the avoidance response in *cat-2* mutants, suggesting that endogenous dopamine is required for the natural response. Further, mutants containing the *dop-4(ok1321)* allele lacking the DOP-4 receptor were not modulated by food, indicating that DOP-4 is required for the acute responses in ASH in the presence of food (Ezcurra et al., 2011). Cell specific RNAi silencing of *dop-4* expression under ASH specific promoters *sra-6* and *gpa-13* led to deficient avoidance, further indicating that *dop-4* is present in the ASH neuron and a candidate for the modulation by dopamine in the presence of food.

Baidya 2014 *et al.* (2014) found that the DOP-1 receptor also plays a part in modulating chemosensory avoidance behaviors. They found that dopamine modulates the avoidance response to octanol, as *cat-2(e1112)* mutants have increased latency in their response to this aversive stimulus. Therefore, dopamine must work in octanol sensing neurons (including ASH), command interneurons, or others that receive input from these neurons. Triple deletion mutants for *dop-1*, *dop-2*, and *dop-3* displayed increased latency similar to the *cat-2* mutants, indicating that these three receptors may function redundantly. In a separate study, Ezcurra *et al.* observed that DOP-1 appears to act in the presence of food to inhibit adaptation responses to copper, although not within the ASH neuron (2016). Mutants lacking a functional copy of *dop-1* showed similar responses to *cat-2* mutants when off food. Rescue of *dop-1* under the

ASH specific promotor *sra-6* did not rescue responses, although rescue of *dop-1* under its own promotor did. These results suggest that *dop-1* might function in neurons other than ASH, possibly the AUA neurons (Ezcurra et al., 2016).

Taken altogether, these behavioral results indicate that DOP-1 and DOP-4, and perhaps others, are responsible for dopamine modulation of avoidance responses to chemical repellants, mediated by the ASH neuron and connecting interneurons. Previous studies investigating *dop-1* and *dop-4* reporter gene expression, however, suggested that neither of the receptors are expressed in the ASH neuron (Sugiura et al., 2005; Tsalik et al., 2003).

dop-1::gfp and *dop-4::gfp* Expression in Head Neurons

Expression of *dop-1::gfp* reporter constructs have shown differing expression patterns in different studies. Tsalik *et al.* found consistent *dop-1::gfp* expression in the RIM interneuron class and weak, inconsistent expression in other unidentified cells (Tsalik et al., 2003). It was noted that alternative reporter fusions with additional sequences of promoter included have shown expression in additional unidentified head neurons. Sanyal *et al.* found *dop-1::gfp* expression in the PLM, PHC, and ALM mechanosensory neurons, ASI sensory neurons, as well as tentative assignments to the AUA, RIB, and RIM interneurons. Low intensity of fluorescence made assignments to some head neurons difficult (Sanyal et al., 2004). Meanwhile, Chase *et al.* found *dop-1::gfp* expression in several head neurons, though these neurons were not individually identified (Chase et al., 2004). It was acknowledged that they found more neurons with

dop-1::gfp expression than previously described reporters, likely due to additional promoter sequence included in their construct.

Sugiura *et al.* 2005 found consistent *dop-4::gfp* expression in neurons ASG, AVL, CAN, and PQR, with inconsistent and weak expression in other unidentified head neurons (Sugiura *et al.*, 2005). Thus, limitations in classic gene editing techniques may have restricted our observations of expression profiles of dopamine receptors to date by the variability in constructs as well as unreliable signal, making identification of individual neurons difficult. How does this variability occur?

Classic transgenic techniques, such as those used originally to visualize the locations of dopamine receptors, involve injecting plasmid DNA containing promoter-reporter gene fusions into *C. elegans* gonads, which are taken up by developing embryos and then formed into episomal tandem DNA repeats known as extrachromosomal arrays to be expressed in offspring (Fay, 2013; Mello *et al.*, 1991). However, these reporter genes may exhibit different expression patterns than endogenous genes as the promoter fragments are removed from their normal chromosomal context and thus may lack key *cis*-acting elements or may have altered chromatin structure essential for normal gene expression. It is not uncommon to observe differing expression patterns due to differences in the length of promoter sequences used (Chase *et al.*, 2004; Sanyal *et al.*, 2004; Suo *et al.*, 2003; Tsalik *et al.*, 2003).

Classic Gene Editing Techniques in *Caenorhabditis elegans*

These problems might be solved with a gene targeting approach.

However, gene targeting techniques utilizing transposons (such as Tc1, *Mos1*) or nucleases (such as zinc finger nucleases or TALENs) are limited in their specificity, involve complex customization, and may require specialized *C. elegans* strains. Transposons, such as *Mos1*, are sequences of DNA which may move in the genome with the aid of a transposase. Following excision of the transposon and a double stranded break, a transgene providing a repair template may introduce the desired edit. The most commonly used transposon, *Mos1*, is in fact not endogenous to *C. elegans*, but rather to *Drosophila*. Transgenic strains of *C. elegans* containing a transposon sequence near or in the target gene must be identified and requested through the NemaGENETAG Consortium. Further, these gene excision events are exceedingly rare (Robert & Bessereau, 2007).

Zinc finger nucleases (ZFNs) are chimeric protein complexes formed of two or more zinc finger domains, each zinc finger domain recognizing a three-nucleotide sequence, joined with a *Fok1* restriction enzyme, which cuts at the end of the recognized sequence. By using two zinc finger nucleases in tandem, a sequence of up to 18 nucleotides may be used to specify a target site. Zinc finger nucleases require extensive modification, becoming costly.

TALENs function similarly to ZFNs, however, are comprised of TAL domains fused to a *Fok1* enzyme rather than zinc fingers. Each TAL domain is

specific to one nucleotide, so the combination of TAL domains is more easily modified. Germline transmission using either approach is very rare.

CRISPR/Cas9 as a Precision Gene Editing Tool

The Clustered Regularly Interspersed Short Palindromic Repeats

(CRISPR) / CRISPR-associated (Cas) system was originally discovered as a defense mechanism in archaea and bacteria as an adaptive immune response to invading bacteriophages and plasmids. Various teams noticed sporadic, repeated sequences in halophilic archaea and bacteria (Mojica et al., 1995). Over time it was noticed that these repeat sequences were well conserved, and they began to be referred to as CRISPR (Jansen et al., 2002). Soon after, segments of the sequences were identified as being of foreign origin amidst the repeated sequences, and were proposed to provide an adaptive immune function, “keeping a record” of previous invasions (Mojica et al., 2005; Pourcel et al., 2005).

CRISPR/Cas9 is an RNA-protein holoenzyme composed of the Cas9 endonuclease and two segments of RNA, the *trans*-activating CRISPR RNA (tracrRNA) and the CRISPR RNA (crRNA). The clustered regularly interspersed short palindromic repeats encode the RNA components of the functional holoenzyme. The tracrRNA assists in the processing and maturation of crRNA and hybridizes to both the crRNA and Cas9 protein for activation. The crRNA detects sequences in foreign DNA with base-pair complementarity, adjacent to a

short NGG motif known as the protospacer adjacent motif (PAM), to signal destruction by Cas9.

Since its discovery, CRISPR/Cas9 has been adopted for targeted gene editing in various systems, including eukaryotes (Cong et al., 2013). With the advent of the CRISPR/Cas9 method, endogenous loci can be targeted and edited with a great deal of specificity. Targeted editing is achieved by customizing the crRNA sequence to be complementary to virtually any desired target sequence, given it is in proximity to an NGG motif, where the Cas9 protein can create a double-stranded DNA break (DSB) (Jinek et al., 2012). The NGG motif is essential for the crRNA to recognize, as it recognizes and binds to the PAM sequence before recognizing the complementary guide sequence. The crRNA and tracrRNA may be fused with the addition of a linker to form a single guide RNA (sgRNA) (Jinek et al., 2012). Following DSB, repairs can be made through either non-homologous end joining (NHEJ), or by stimulating homology directed repair (HDR) (Cong et al., 2013). NHEJ is error prone and thus usually only used to disrupt coding regions for loss of function mutations. HDR is used to create much more specific and targeted mutations such as point mutations, insertions, or deletions. New sequences can be engineered into the DSB point by simultaneously introducing a repair template DNA that is targeted to the break point by homologous flanking sequences (

Figure 3).

CHAPTER TWO:

MATERIALS AND METHODS

Strategy 1: Oligonucleotide Based Approach

CRISPR Sequence Design

Two crRNAs were designed to target the *dop-1* (5'-ATTCGATGAACGATTTGCAATGG-3') and *dop-4* (5'-ATATAGAGGTCTTCGGCGTTCGG-3') genes, respectively, with online tool CRISPOR and analyzed for specificity, off-target effects, and proximity to intended edit (Concordet & Haeussler, 2018). These crRNA target sequences were utilized in both strategies. For the oligonucleotide-based strategy, Edit-R crRNAs, tracrRNA and Cas9 protein were purchased through Dharmacon.

Plasmids

Plasmid dg353, containing a *C. elegans* optimized mNeonGreen, was a gift from Dominique Glauser and Allele Biotechnology & Pharmaceuticals (Hostettler et al., 2017; Shaner et al., 2013). pCFJ90 - Pmyo-2::mCherry::unc-54utr was a gift from Erik Jorgensen (Addgene plasmid # 19327 ; <http://n2t.net/addgene:19327> ; RRID:Addgene_19327). Plasmids were verified by diagnostic digest.

PCR

PCR was performed using Thermo Scientific Phusion High-Fidelity PCR Master Mix. (See Table 2 for list of oligonucleotides used in Strategy 1.) Reagents were assembled as recommended by Paix et al. 2016 supplemental

protocol. Thermocycler conditions for mNeonGreen are as follows: initial denature for 2 minutes at 98°C, 30 cycles of denaturing at 98°C for 30 seconds, annealing at 62°C for 15 seconds, extension at 70°C for 25 seconds, with a final extension step of 70°C for 2 minutes. Thermocycler conditions for mCherry are as follows: initial denature for 2 minutes at 98°C, 30 cycles of denaturing at 98°C for 30 seconds, annealing at 62°C for 15 seconds, extension at 70°C for 60 seconds, with a final extension step of 70°C for 2 minutes. PCR products were confirmed by 1% agarose gel electrophoresis and purified using Promega Wizard® SV Gel and PCR Clean-up System.

Four sets of ssODNs were designed to bridge each mNeonGreen and mCherry to each *dop-1* and *dop-4*. ssODNs were purchased from IDT or Invitrogen. Co-conversion reagents were designed to also edit the *dpy-10* locus to assist in screening for edits made (Arribere et al., 2014). The *dpy-10* crRNA (5'-GCUACCAUAGGCACCACGAG-3') and repair ssODN (5'-CACTTGAACCTTCAATACGGCAAGATGAGAATGACTGGAAACCGTACCGCATGCGGTGCCTATGGTAGCGGAGCTTCACATGGCTTCAGACCAACAGCCTAT-3') were used to generate the *dpy-10(cn64)* mutant.

Strains and Culture

Bristol N2 *C. elegans* were used as wildtype and parent strain for all injections in the oligonucleotide-based strategy. Worms were cultured on standard nematode growth media (NGM) agar at 20°C or 25°C as described by (Stiernagle, 2006).

Microinjection

Injection mix was prepared with the following: 12.5 ng/μL Cas9, 1 μg/μL tracrRNA, 0.16 μg/μL *dpy-10* crRNA, 13.75 ng/μL *dpy-10* ssODN, 0.4 μg/μL *dop-1* targeting crRNA, 0.46 pmol/μL mNeonGreen PCR template, ssODN bridging oligonucleotides, KCl, HEPES (Dickinson et al., 2015).

Worms were injected as outlined by (Evans, 2006). Briefly, worms were mounted on injection pad coverslips layered with a small area of agarose. Worms were cleaned of carryover eggs or bacteria in a large drop of halocarbon oil, then affixed to the pad with a small amount of oil. Injection needles were pulled from thin borosilicate microcapillary tubes to a fine point, then filled with injection mix through capillary action. Worms were injected in each branch of the gonad. Following injection, worms were transferred to a recovery NGM plate and supplemented with recovery buffer.

Screening for Edits

Candidates were screened for identifiable phenotypes, with heterozygotes (*dpy-10/+*) presenting a Roller (Rol) phenotype and homozygotes (*dpy-10/dpy-10*) presenting as Dumpy (Dpy) (see Figure 11). Heterozygous Rol candidates were screened by PCR for both out-of-frame and in-frame insertions utilizing a combination of PCR primers external and internal to the fluorescent protein coding sequence and locus of interest. A pair of primers internal to the FP coding sequence indicated correct insertion of GFP at some location within the genome. Further, a set of primers containing one forward primer external to the target

locus and one internal to the FP confirmed correct insertion of GFP at the gene of interest. Worms positively screened by PCR were visualized using epifluorescence microscopy.

Worm Lysis

C. elegans genomic DNA was isolated by application of MPGC buffer (21 mM Na₂HPO₄, 11 mM KH₂PO₄, 4.3 mM NaCl, 9.3 mM NH₄Cl, 16 mM PEG8000, 1.6 mL of 5 mg/mL cholesterol in 100% ethanol), freezing at -80° C for one hour, addition of worm lysis buffer (10 mM Tris-HCl, 50 mM KCl, 2.5 mM MgCl₂, 0.45% Tween 20, 0.05% gelatin), and 10 mg/ml proteinase K, and incubating at 60° C for one hour followed by 30 minute heat inactivation at 95° C.

Strategy 2: Plasmid-Based Approach

Plasmids

pDD162 (Peft-3::Cas9 + Empty sgRNA) was a gift from Bob Goldstein (Addgene plasmid # 47549 ; <http://n2t.net/addgene:47549> ; RRID:Addgene_47549). pDD282 was a gift from Bob Goldstein (Addgene plasmid # 66823 ; <http://n2t.net/addgene:66823> ; RRID:Addgene_66823).

Recombinant DNA / Plasmid Constructs

Oligonucleotide primers were designed using ApE software (Davis, n.d.). Primers were designed to insert guide sequences targeting each *dop-1* and *dop-4* into vector plasmid pDD162, using the same CRISPR target sequences as described in Strategy 1. (See Table 3 for list of oligonucleotides used in Strategy

2.) Plasmids targeting CRISPR / Cas9 components to *dop-1* and *dop-4* were edited using the NEB Site Directed Mutagenesis Kit (NEB, Ipswich, MA).

To build repair templates that would assist in HDR, another set of primers were designed to build homology arms with homology to each genomic *dop-1* and *dop-4* into plasmid pDD282, building pZY24 and pZY25, respectively.

Plasmids providing the fluorescent protein repair template were edited using the NEBuilder HiFi DNA Assembly Master Mix (NEB, Ipswich, MA).

Sequencing

Sequencing of plasmids and PCR products was provided by Genewiz. Plasmid candidates were sequenced by Genewiz using primer (5'- GTTATGAAATGCCTACACCCTCTC -3'), and analyzed through plasmid editing software to scan for target sequences. Whole plasmid sequencing was performed by Plasmidsaurus (Plasmidsaurus, Eugene, OR).

Strains and Culture

Bristol N2 *C. elegans* were used as wildtype and parent strain for injections. For experiments using the CRISPR Cas9 integrated transgene, *C. elegans* strain EG9882 were used for injections. Worms were cultured on standard NGM agar as described (Stiernagle, 2006). Strain CGC102 served as a reference for visualizing RFP and *sqt-1* phenotypes. Some strains were provided by the CGC, which is funded by NIH Office of Research Infrastructure Programs (P40 OD010440).

Worm Lysis

Worms were lysed using the Sigma Extract-N-Amp tissue kit (Madhu et al., 2022).

Microinjection

Injection mix was prepared with 50 ng/μl CRISPR Cas9 encoding plasmid, 50 ng/μl repair template plasmid, and 2.5 ng/μl fluorescent co-injection marker (Dickinson et al., 2015). Worms were injected as outlined (Evans, 2006). Injected worms were recovered to fresh NGM plates with 3 injected P0s per plate to grow at 20°C or 25°C for 3 – 4 days.

Selection Strategy

In addition to the GFP coding sequence, the repair template plasmid includes a removable selection marker strategy. The plasmid includes a self-excising cassette (SEC) encoding hygromycin resistance, Cre recombinase under control of a *hsp* promoter, and flanking *loxP* sites (

Figure 5). Following injection, worms were grown at 20°C or 25°C for 3-4 days. At that time, plates with F1 offspring were applied a prepared solution of hygromycin to a final concentration of 250 μg/mL to select for hygromycin resistance conferred by the repair template SEC. Candidates for successful edits 1) survived hygromycin selection; 2) exhibited the Rol phenotype conferred by *sqt-1*; and 3) lacked RFP expression indicating formation of extrachromosomal arrays. Candidates that met all three criteria were singled to new NGM plates and grown at 20°C or 25°C for 3-4 days.

Self-Excising Cassette Removal

Following isolation of candidate knock in lines, three plates from each line (each containing 6-8 L1 or L2 stage animals) were heat shocked at 40°C for 4 hours, activating expression of Cre recombinase and thereby removing the selection SEC. Worms lacking the Rol phenotype and RFP expression following heat shock were singled to new plates to be observed for Mendelian inheritance.

CHAPTER THREE:

RESULTS

Strategy Overview

To perform any kind of CRISPR experiment, a guide sequence targeting a locus for double strand break must be chosen. The CRISPR guide sequences in this experiment were selected through the online tool CRISPOR, which searches the specified model organism genome for possible target sequences adjacent to NGG motifs and assigns scores based on specificity and potential off-target sites (Concordet & Haeussler, 2018). In consideration of these factors, and proximity to the desired in-frame N-terminal fusion construct, target sequences were chosen for each *dop-1* and *dop-4*, with scores of 96 and 100 respectively, with 100 being best. Each target sequence was located within the beginning of the respective coding sequence being targeted and ensured in-frame insertions.

Following CRISPR/Cas9 induced double stranded breaks, edits can be made by various strategies. Here, two different strategies were utilized to increase the likelihood of success: introducing linearized oligonucleotide repair templates, and introducing the repair template as plasmids (

Figure 4).

Though the strategies differ in the constructs and reagents, each strategy necessitates microinjections into adult N2 *C. elegans* gonads. To develop proficiency in microinjection, injections were performed using plasmid DNA to create transgenic lines using standard approaches (Mello et al., 1991). The pRF4

plasmid contains the dominant *rol-6(su1006)* mutant collagen allele, which produces a twisted cuticle that induces animals to crawl in a corkscrew motion (Mello et al., 1991). Successful microinjection resulted in the formation of extrachromosomal arrays and conferred a dominant Rol phenotype (Figure 8).

Strategy 1: Oligonucleotide Based Approach

In this approach, the CRISPR components (crRNA, tracrRNA, Cas9 protein, and oligonucleotide repair templates) were assembled and injected *in situ* (Figure 4A). The repair template consists of a dsDNA encoding the fluorescent protein, along with flanking oligonucleotides containing homology to both the target locus and the fluorescent reporter. Simultaneously, a co-CRISPR strategy to introduce a dominant *dpy-10* mutant allele edit was utilized to aid in identifying transformants. The advantages of this approach include no cloning, more flexibility in design, and a supposed higher rate of editing efficiency with some claims of editing efficiency as high as 50%, which would preclude the need for any kind of selection scheme.

To assess the efficacy of the CRISPR/Cas9 reagents, preliminary injections with CRISPR were performed targeting only the *dpy-10* locus that would serve as the co-CRISPR marker in the final editing mix. This co-CRISPR edit would confer the dominant *dpy-10(cn64)* mutation into the endogenous *dpy-10* locus that induces a discernably squat and fat phenotype referred to as Dpy

(to describe a short Dumpy body). Heterozygous edits (*dpy-10/+*) confer a Rol phenotype, while homozygous edits (*dpy-10/dpy-10*) are Dpy (

Figure 8). Of the 20 P0 worms in preliminary *dpy-10* experiments, there were 6 F1 Rol and 4 Dpy. F1 progeny gave rise to F2 offspring following Mendelian patterns of inheritance, indicating that edits successfully integrated into the germline.

To generate the linear dsDNA repair templates necessary for the final construct, genes coding for two separate fluorescent proteins, mNeonGreen (mNG) and mCherry, were chosen. The mCherry coding sequence plus the *unc-54* 3' UTR was chosen as an alternative construct to mNeonGreen to assess whether introducing solely a fluorescent protein coding sequence would be effective, or whether including an endogenous 3' UTR would aid in final packaging and expression. A concern with this approach is that a larger size repair template may limit editing efficiency. The linear repair templates were produced by PCR amplifying the genes encoding the fluorescent proteins from their respective plasmids and confirmed by gel electrophoresis to be of the correct size (

Figure 6). Bridging oligonucleotides were designed to contain homology to both the target loci and the dsDNA repair template to facilitate HDR.

After assembling all necessary reagents, injections of 64 P0 animals with *mNG::dop-1* showed 11 F1 Rol and 15 Dpy out of a total of 1298 F1. This data demonstrates an editing efficiency of 2% for the *dpy-10* locus. Of these,

candidate F1s were PCR interrogated for both targeted or off-target *mNG* insertions, but none yielded edits at the *dop-1* locus or elsewhere. With a low editing efficiency and lack of selection for rare events, this method did not seem to be feasible. Thus, priority was given towards utilizing Strategy 2.

Strategy 2: Plasmid Based Approach

An alternative approach used plasmids to express the CRISPR Cas9 components as well as a repair template plasmid in the injection mix (Figure 4B). This approach may be more reliable for integrations of larger edits such as fluorescent proteins and selection markers (Dickinson et al., 2015). The advantage of this strategy includes an elegant selection strategy, as described in Chapter Two, that allows for selection of rare events rather than brute-force screening. This selection strategy confers an easily identifiable and removable self-excising cassette (SEC; see Introduction and Materials and Methods), which contains a dominant *sqt-1* mutant allele, a hygromycin resistance gene, and heat-shock inducible Cre recombinase gene.

To build the plasmids encoding CRISPR components targeting *dop-1* and *dop-4*, sequences targeting their respective target loci were added to the vector by site directed mutagenesis. Following confirmation of PCR products of the expected sizes (

Figure 7), products were ligated and transformed into chemically competent cells. Twelve candidate colonies for each edit were purified and sent for Sanger sequencing. Ten candidates were confirmed to carry the crRNA

sequence targeting *dop-1* and nine candidates were confirmed to carry the crRNA sequence targeting *dop-4*. Whole plasmid sequencing further confirmed no additional mutations in these plasmids.

To assist in plasmid-based homology directed repair (HDR) as described (Dickinson et al., 2015), primers were designed to build homology arms corresponding to each *dop-1* and *dop-4* to the repair template vector. Homology arms 500-600 bp in length were generated by PCR, utilizing *C. elegans* wildtype genomic DNA as template. Following construction of homology arms by PCR, these fragments were inserted into the vector plasmid by Gibson assembly, building candidate plasmids with homology to *dop-1* and to *dop-4*, respectively. Following Gibson assembly, candidate colonies were isolated for *gfp::dop-1* and *gfp::dop-4*. Again, whole plasmid sequencing further confirmed that these constructed plasmids contained the correct sequences with no errors.

N2 adult hermaphrodite P0 worms were injected with the CRISPR Cas9 encoding plasmid and repair template plasmid targeting *dop-1*. Also included was a plasmid encoding a red fluorescent protein reporter gene under the control of a pharyngeal muscle cell promoter (Dickinson et al., 2015), with no homology to the target locus. Three to four days later, plates containing F1 offspring of injected worms were treated with hygromycin to test for presence of selectable markers conferred by the SEC in the repair template plasmid. In addition to hygromycin resistance, the SEC encodes a dominant *sqt-1* marker that confers a Rol phenotype. Candidates of successful edits exhibited the Rol phenotype and

survived selection with hygromycin. Importantly, candidates also lacked expression of red fluorescent protein (RFP). Expression of RFP in the pharynx would indicate formation of extrachromosomal arrays as the *rfp* reporter plasmid contained no homology to the target locus and thus would not be integrated. This is an important counter screening measure, as the hygromycin resistance and mutant *sqt-1* phenotypes would still be expressed from extrachromosomal arrays. Thus, although some candidates could be Rol and hygromycin resistant, expression of RFP would indicate that this was through the formation of extrachromosomal arrays, not our CRISPR editing strategy.

Candidate Rol, hygromycin-resistant, RFP-negative worms were singled to new, hygromycin-free NGM plates to observe for Mendelian inheritance patterns. Seven candidate lines with a homozygous Rol segregation pattern were identified and maintained; these lines were named ZY60 through ZY66. Each of these lines were lysed and PCR interrogated for the hygromycin resistance gene, as well as GFP insertion at the *dop-1* locus. PCR found three of the seven candidate lines, ZY64 - ZY66, to be positive for both the hygromycin resistance gene and *gfp::dop-1* (

Figure 10). Sanger sequencing of the respective PCR products found that, of these three lines, all three lines had the correct, in-frame insertion of GFP with no introduced errors (Figure 12).

Subpopulations of the three candidate lines that were positive for hygromycin resistance as well as the *gfp::dop-1* insert were then heat shocked to

remove the self-excising cassette (SEC) by heat shock induced CreLox recombination. Following heat shock, worms that lost the Rol phenotype and presented as wild type were singled to individual plates to observe inheritance patterns (

Figure 11). All three of these candidate lines lost the Rol phenotype. Further, these lines were treated with hygromycin once again and were now found to be sensitive to hygromycin, ostensibly after excision of the selection marker in the SEC following heat shock. PCR using a primer set with one primer upstream of the *dop-1* integration site and the other primer located with the *gfp* coding sequence showed that candidate lines ZY64, ZY65, and ZY66 contained the *gfp::dop-1* insertion into the chromosome after heat shock (Figure 12). Sanger sequencing confirmed that all 3 lines maintained the *gfp::dop-1* in-frame insertion sequence following heat shock (

Figure 13).

Fluorescence imaging of worms from these lines, both before and after heat shock, showed only faint autofluorescence in the gut and no detectable fluorescence in the nerve net or ventral nerve cord (

Figure 14). From expression studies, we would expect to see *dop-1* expression in head neurons such as AIZ, ALM, ALN, and AUA, and in ventral cord motor neurons such as DA9, VA neurons (Sanyal et al., 2004; Tsalik et al., 2003). However, we did not see any detectable expression here.

CHAPTER FOUR:

DISCUSSION

The goal of this project was to use CRISPR Cas9 to build a fluorescent reporter gene to identify the expression pattern of the dopamine receptors *dop-1* and *dop-4* in *Caenorhabditis elegans*, with particular attention to the neurons involved in the chemosensory avoidance pathway. Classic transgenic techniques used to build fluorescent reporters in *C. elegans* involved selecting a section of upstream sequence thought to be the promoter of the target gene, building a promoter-reporter fusion plasmid, and microinjecting this plasmid into the animal, resulting in the formation of extrachromosomal arrays. Due to the nature of extrachromosomal arrays containing several hundred copies of the construct, the reporter is over-expressed. Further, due to the nature of the promoter-reporter construct, the segment of promoter sequence used may not be truly representative of the full promoter in terms of chromatin context and all *cis*-regulatory elements. CRISPR Cas9 is impressive in its power to generate precise edits right at the target genomic locus, thus potentially allowing analysis of the endogenous expression pattern.

Here, a total of three CRISPR Cas9 editing strategies were utilized. The first, oligonucleotide based strategy yielded low editing efficiency. Whereas other groups had claims of editing efficiency from 5% to as high as 50% of *dpy-10* edited worms containing an edit at the target locus as well, here we found none (Paix et al., 2015). Higher editing efficiency using this strategy is supposed to

preclude the need for selection. However, we did not observe any edits, which might suggest a lower editing efficiency. Thus, it would have been necessary to inject, screen, and verify a very large number of worms to obtain our desired edit. The low editing efficiency we observed may be due to low activity of our chosen target gRNA.

Other groups are working on optimizing CRISPR Cas9 editing strategies with RNP and oligonucleotide repair template delivery following difficulty reproducing the proclaimed editing efficiency. Using a sgRNA rather than crRNA and tracrRNA (which must anneal together) may have higher editing efficiency, as unannealed tracrRNA may form tetrameric complexes (Prior et al., 2017). In their protocol, Prior et al. found success with reduced concentration of injected RNP complex to reduce off-target effects, as well as utilizing a transient fluorescent protein injection marker, rather than a co-CRISPR strategy that introduces a second DSB.

In terms of the oligonucleotide repair template, one group developed a nested CRISPR protocol, in which the desired edit is implemented in two steps (Vicencio et al., 2019). In the first step, a ssODN repair template containing proximal and distal segments of the desired gene is inserted into the locus of interest. This homology facilitates the HDR of a dsDNA repair template, which integrates the remainder of the gene to be inserted in the second step. Another group found more success by using dsDNA PCR product repair templates with ssDNA overhangs (Dokshin et al., 2018). Yet another group found that heating

and cooling the dsDNA templates greatly increased editing efficiency. (Ghanta & Mello, 2020).

In comparison, the plasmid-based strategy involved the use of plasmids designed to encode CRISPR Cas9 as well as the repair template. The repair template plasmid included 500–600 bp homology arms to facilitate homologous recombination, much longer than that supported by the oligonucleotide strategy. Additionally, the repair template plasmid included a selection marker, which made identifying candidates for edits much more efficient by selecting for rare events. This method further had the benefit of allowing facile removal of the SEC by heat shock-induced Cre recombinase expression, leaving only the desired edit.

One variation to this protocol involved injections into a *C. elegans* line containing an integrated transgene encoding the Cas9 protein. This protocol claimed the benefits of less reagents to inject, as well as increased editing efficiency due to reduced germline silencing of plasmid-born Cas9. We obtained this line and attempted to generate integrants with it (Schwartz et al., 2021). This transgenic line had the tendency to become a “bag of worms”, a phenotype in which defective egg laying leads to eggs hatching inside the parent. This may have been due to remaining features of the transgenic line, created by using *Mos1*, or possible off-target CRISPR effects. This phenotype gave considerable difficulty in performing microinjections of P0 adults, as well as difficulty in observing the phenotypes of F1 offspring. After injections of over 50 P0 animals

of this transgenic line, we obtained no discernable Rol offspring. Therefore, injections were resumed using N2 worms.

Resuming the plasmid-based strategy with injections into N2 worms ultimately established seven candidate lines, of which three lines were verified by PCR and Sanger sequencing to have the *gfp::dop-1* edit. Fluorescence imaging showed only faint autofluorescence in the gut and no detectable fluorescence in the head ganglia/nerve net or ventral nerve chord, where we would expect to be detect *dop-1* expression (

Figure 14). It may be possible that no fluorescence reporter expression was detected due to errors introduced following repair of the double-strand break. However, this is unlikely, as the protocols used here specifically facilitate homologous recombination rather than non-homologous end joining, which is inherently more mutagenic. Homologous recombination is a high-fidelity repair route which uses strand invasion to find sequences of homology to serve as template and rebuild the strands. With the use of a template with homology and the high fidelity of DNA polymerase, it is unlikely that any errors were introduced. We also assessed multiple independent lines. We confirmed this through Sanger sequencing of the edited lines and showed that in each case the inserted sequence was in-frame and contained no erroneously introduced errors.

It may be possible that, despite sequencing showing the presence of the correct insert in the genome, the expression of the reporter is being silenced at some level. One possible mechanism of silencing may be germline silencing

(Schwartz et al., 2021). With classical transgenesis which generates extrachromosomal arrays with tandem repeats, transgenes are often silenced due to the high copy number. Silencing for this reason is unlikely, as this experiment created a single copy transgene, demonstrating reduced copy number and thus less foreign elements to be recognized and silenced. Another possible mechanism of silencing is nonsense-mediated RNA decay, wherein mRNAs containing a premature translation-termination codon are degraded (Mango, 2001). This scenario is unlikely as the edit introduced creates a gene fusion of *gfp::dop-1*, maintaining the endogenous *dop-1* stop codon and UTR. Further, the inclusion of synthetic *C. elegans* introns within the GFP coding sequence should reduce the possibility of nonsense-mediated mRNA decay.

To assess *dop-1::gfp* expression, the next steps would be to detect expression in ways besides fluorescence. Either a Northern blot or reverse-transcription PCR would show transcription of the reporter gene into mRNA. Another approach to detect expression of the reporter in general would be utilizing Western blot analysis to detect translated protein. While this technique may not provide location of the expressed protein, it may provide evidence that the protein reporter is expressed at any level.

Towards our goal of detecting where the reporter and our gene of interest are being expressed, this may be possible by using in situ hybridization or immunohistochemistry. By using in situ hybridization with an RNA probe for our construct, the location of transcription of the *gfp::dop-1* gene may be examined.

However, in situ hybridization in *C. elegans* has poor spatial resolution. In worms, in situ can provide very generalized regions of expression, however, fixation distorts cellular detail that helps identify individual neurons.

Immunohistochemistry may also localize expression of the reporter protein. The repair template plasmid confers a 3x FLAG tag that would be expressed after excision of the SEC (

Figure 11). By using either an anti-GFP or anti-Flag antibody, immunohistochemistry may show where our construct is expressed.

It may be possible, in fact, the most parsimonious explanation, that fluorescence expression was not observed due to low endogenous expression of the *dop-1* gene. Levels of detection seen here may also be low due to differences in expression in different life stages. The model organism Encyclopedia of DNA Elements (modENCODE) project libraries shows that *dop-1* is generally more highly expressed in developing embryo and L1 stage. In the dauer larva stage, there was an average expression of 7.07 fragments per kilobase of transcript per million (FPKM) and an average expression of 12.4 FPKM in L1 larva (Gerstein et al., 2010).

Although we were not able to detect fluorescence here, single cell RNA sequencing data may help guide us where to look more specifically for fluorescence when confocal microscopy is available. The *dop-1* gene may not be expressed in the ASH neuron but in connected interneurons involved in the chemosensory avoidance pathway (

Figure 1). According to the *C. elegans* Neuronal Expression Map and Network (CeNGEN) consortium, single cell RNA sequencing shows that neither *dop-1* or *dop-4* is expressed in ASH neurons (Hammarlund et al., 2018). However, *dop-1* is expressed in the AUA neuron at a level of 88.15 transcripts per million (TPM), in the AVA neuron at 230.57 TPM, in AVB at 97.02 TPM, and in AVD at 118.20 TPM. For comparison, *ser-7* (a receptor for another biogenic amine neurotransmitter - serotonin) is expressed in the AUA neuron at a level of 294.50 TPM. Interestingly, a glutamate receptor *glr-4* is more widely expressed in the chemosensory circuit of interest here –in AUA at 44.26 TPM, in AVA at 183.54 TPM, AVB at 85.84 TPM and AVD 173.77 TPM. Glutamate receptors mediate a majority of the excitatory neurotransmitter signaling in vertebrate central nervous systems (P. Brockie, 2006). For another point of comparison, a widely expressed histone encoding gene *his-72* is highly expressed in all neurons in the circuit - in ASH at 230.29 TPM, in AUA at 477.79 TPM, AVA at 608.28 TPM, AVB at 337.81 TPM. Fluorescence reporter expression for *his-72::gfp* (created as a targeted gene replace similar to the strategies used here) demonstrated bright fluorescence, suggesting that lower expression may be insufficient for detection via GFP reporters. Taken altogether, we hypothesize that *dop-1* had no detectable fluorescence because it is expressed at a relatively low level (**Error! Reference source not found.**).

Although here we focused on creating a *gfp::dop-1* fusion reporter, all necessary reagents were constructed for creating a *gfp::dop-4* construct as well.

While we did not get to examine fluorescence reported expression here, single cell RNA sequencing data may point us to focus in the right direction in future studies. The CeNGEN consortium shows that there is no expression of *dop-4* in the AUA or AVD interneurons, but there is expression in the AVA neuron at 45.47 TPM and in the AVB neuron at 82.16 TPM. Future work capitalizing on the approach used here may still answer our question – in which neurons are *dop-1* and *dop-4* expressed?

When available, confocal microscopy may provide higher signal-to-noise ratio compared to wide-field fluorescence microscopy, allowing better detection of low levels of fluorescence. If GFP expression alone were still too low to be detected, immunofluorescence with anti-GFP or anti-FLAG antibodies may enhance the fluorescence signal enough to identify the location of expression. Alternatively, the same overall editing strategy could be used to build the repair template plasmid with mNeonGreen or another fluorescent protein that is brighter and/or more resistant to photobleaching and thus might provide more detectable fluorescence. At the time of the start of this project, a vector plasmid with mNeonGreen was not available, though there are now. Otherwise, using a non-fluorescent reporter such as the *lacZ* gene encoding β -galactosidase may demonstrate expression without the limitations of fluorescent proteins. As β -galactosidase is an enzyme, it would report expression without being susceptible to photobleaching as with fluorescent protein reporters or immunofluorescence. In fact, given more time and substrate to develop color, β -galactosidase may

enhance a weaker signal. The main limitation to this method is again fixation of the animal which may distort structures that would aid in identifying neurons. Optimistically, with the availability of confocal microscopy and the constructs for targeting both genes built, we may yet determine the expression pattern of the *dop-1* and *dop-4* genes.

Here, we developed a successful CRISPR system of integrating reporter transgenes at the endogenous locus of the gene of interest. While our *gfp::dop-1* transgene did not result in detectable fluorescence, the strategies used here may work using other gRNAs, for other loci, or using other fluorescent reporters. The constructs and workflow created here laid the groundwork for this technique in the lab. Future experiments using either of these strategies need only modify and apply the constructs created here.

APPENDIX A:

FIGURES

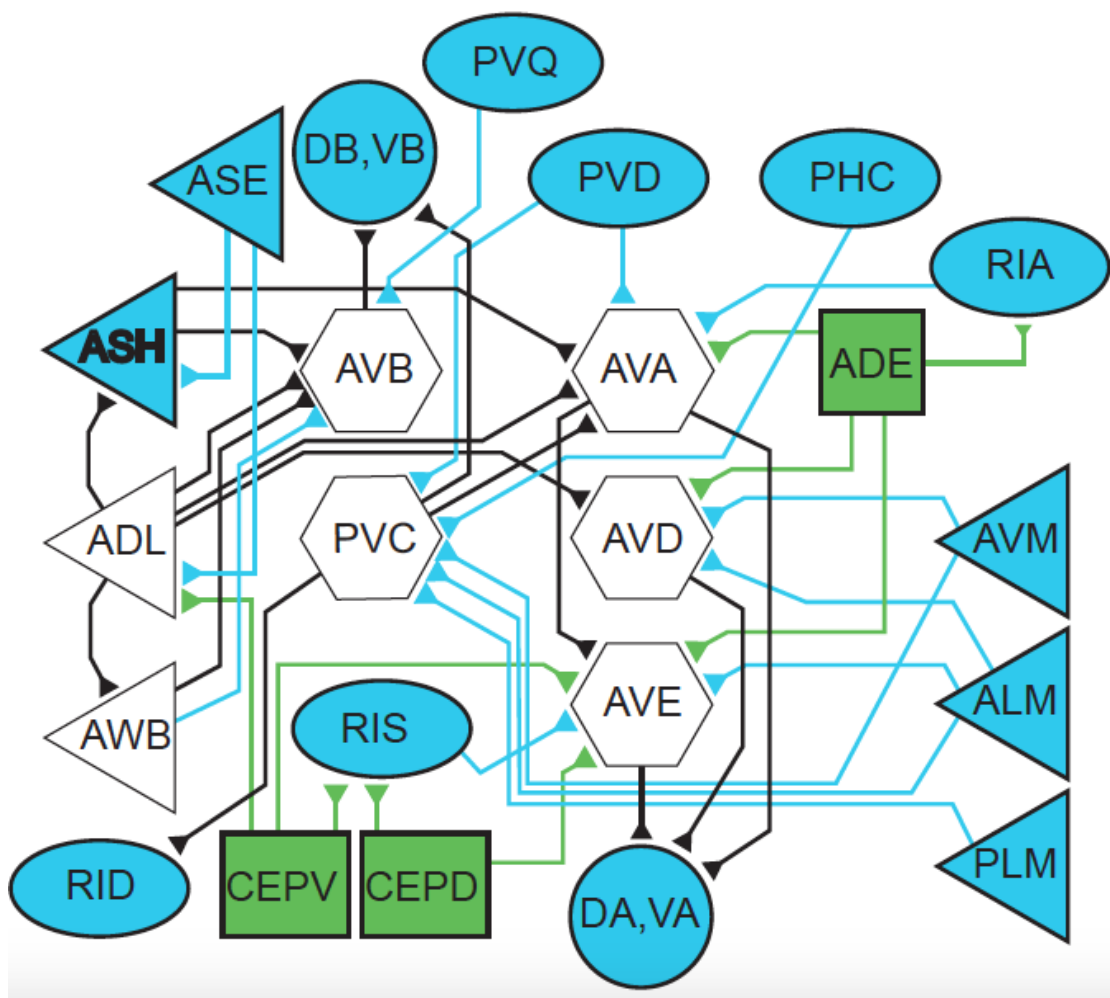


Figure 1. DA connectivity map. Triangles represent sensory neurons, hexagons represent interneurons, squares are dopamine producing, and circles are motor neurons. Shapes in blue contain one or more DA receptors, shapes in green are DA producing.

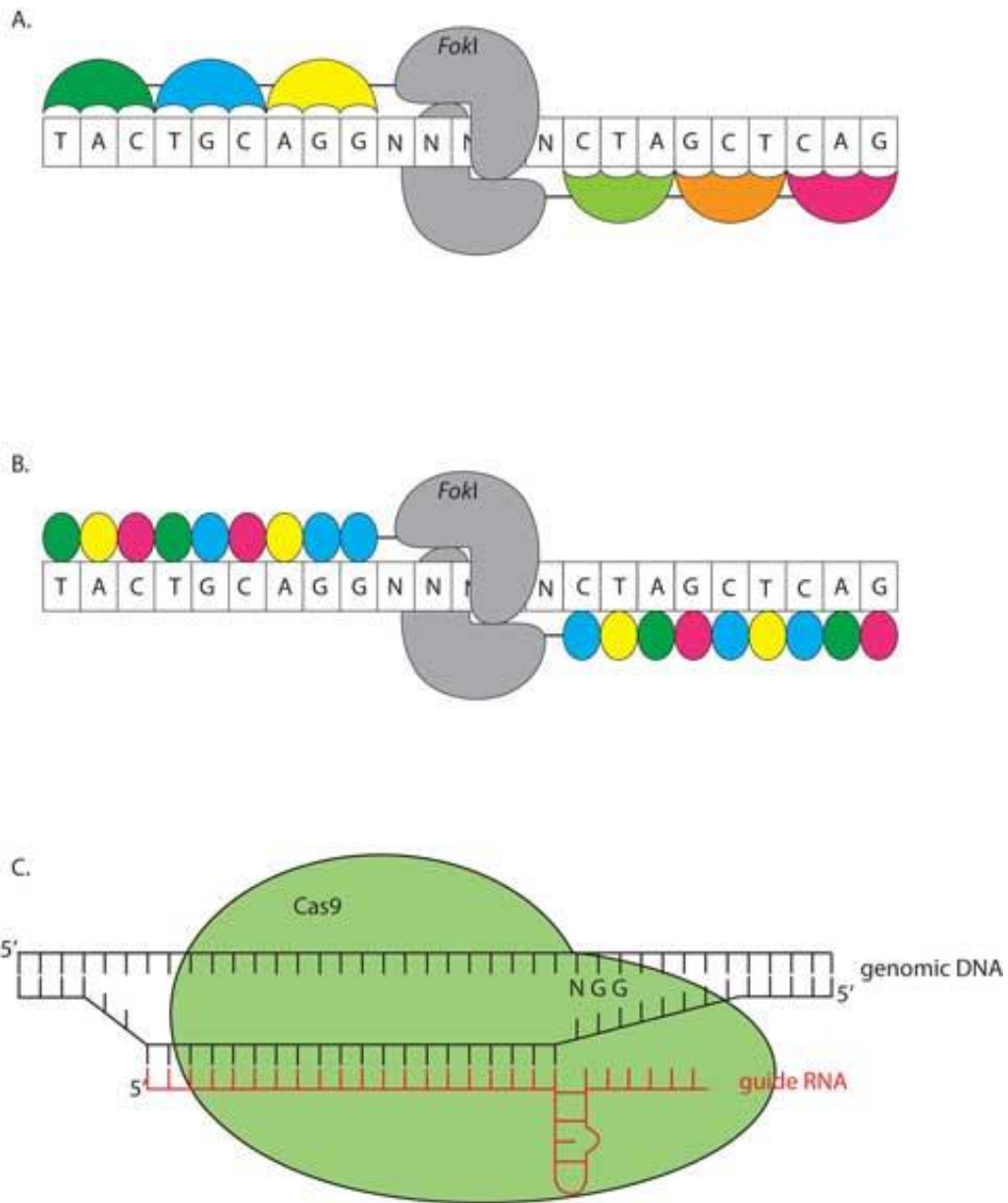


Figure 2. Comparison of Zinc Finger Nucleases (ZFNs), (TALENs), and CRISPR.
From Wormbook, Forward and Reverse Mutagenesis in *C. elegans*.

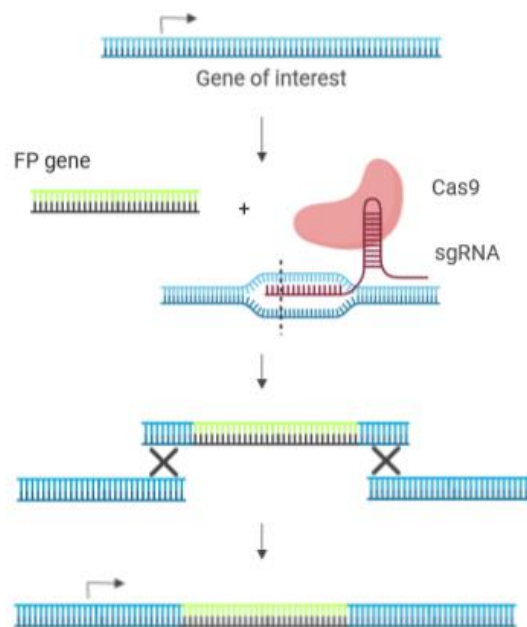


Figure 3. Schematic showing general CRISPR knock-in outline. Genomic locus for target gene of interest shown in blue, CRISPR Cas9 ribonucleoprotein complex shown in red, fluorescent protein coding sequence shown in green. Through sequence customization of the crRNA, in this illustration depicted as the sgRNA, Cas9 finds sequence complementary to the target sequence and creates a DSB. Following DSB, a repair template containing a fluorescent protein coding gene is introduced and inserted through homology, indicated by X's aligning FP to genomic locus. Created with BioRender.com.

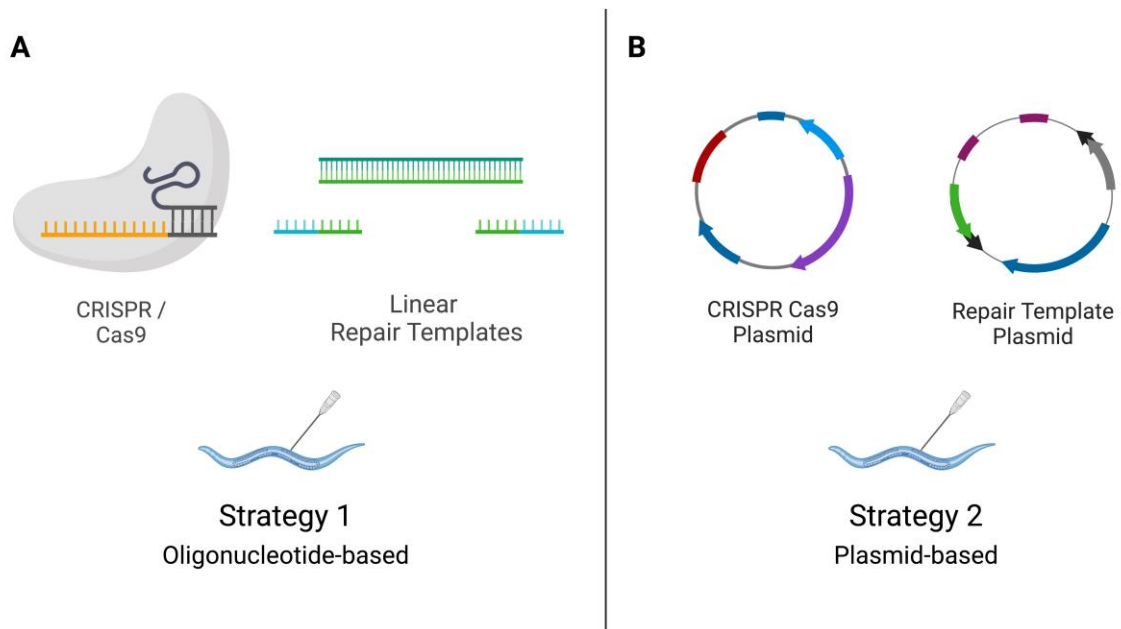


Figure 4. Schematic showing editing strategies used in this experiment. (A) Strategy 1 uses direct injection of *in vitro* assembled CRISPR Cas9 components, with PCR repair templates and bridging ssODNs. (B) Strategy 2 uses plasmid-based expression of CRISPR Cas9 components as well as repair templates.

Created with BioRender.com.



Figure 5. Schematics of the plasmids constructed in Strategy 2. (Top) The pDD162 vector encoding CRISPR Cas9, with an empty gRNA scaffold. Site Directed Mutagenesis would add the *dop-1* and *dop-4* guide sequences, building

plasmids pZY22 and pZY23. (Bottom) The pDD282 vector encoding GFP and the removable SEC. PCR would amplify regions of the *dop-1* or *dop-4* gene at two locations, building the 5' and 3' homology arms (HAs). Gibson Assembly would insert the HAs, building plasmids pZY24 and pZY25, respectively. Created with BioRender.com.

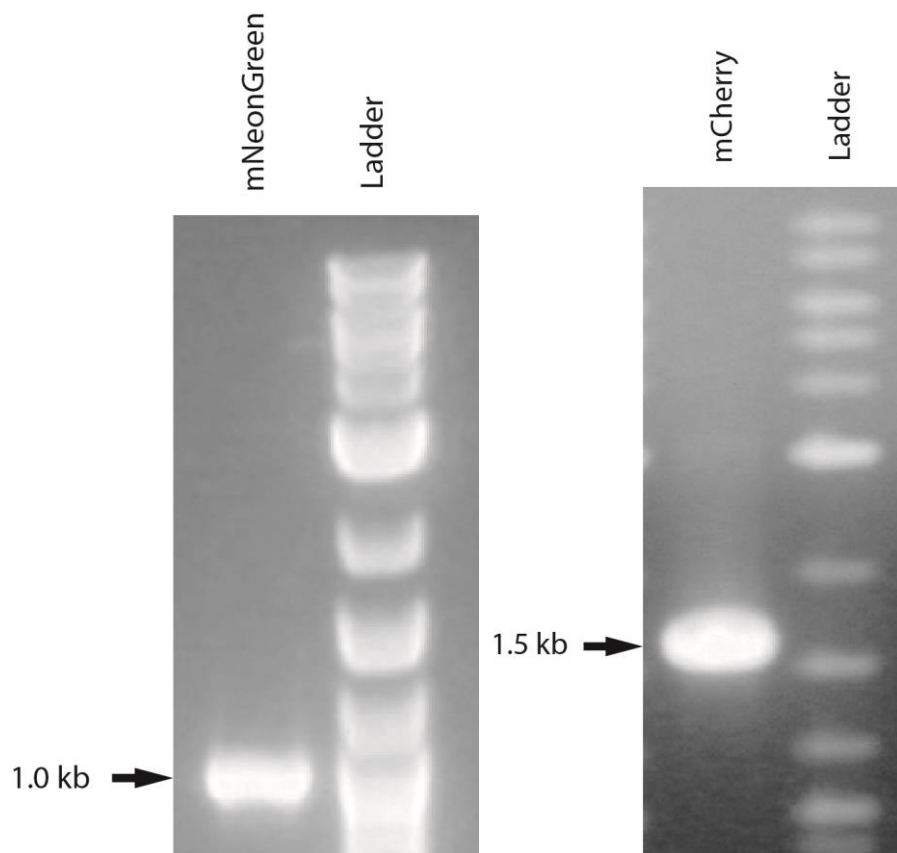


Figure 6. PCR generated fragments encoding mNG and mCherry of the correct sizes. 1% gel electrophoresis of mNeonGreen (mNG) and mCherry + *unc-54* 3' UTR (mCh) PCR products to be used as repair templates in Strategy 1. These repair templates can be used for multiple experiments, using ssODNs to facilitate HDR targeting different loci.

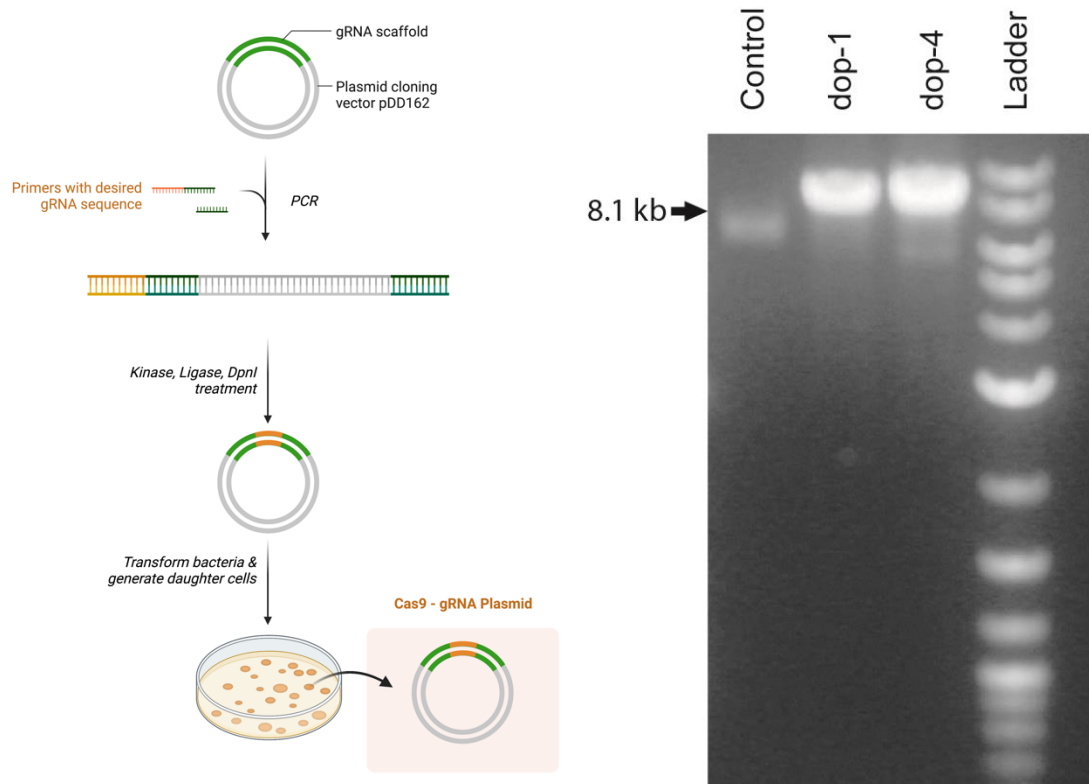


Figure 7. Site Directed Mutagenesis inserted gRNA sequences targeting *dop-1* and *dop-4* into the CRISPR Cas9 vector plasmid. (Left panel) Figure of Site Directed Mutagenesis strategy. Primers containing homology to the vector plasmid and the desired gRNA to be inserted are used to PCR amplify the vector, building in the target gRNA. Kinase, Ligase, and DpnI treatment circularize the plasmid and remove template. Plasmid is then transformed into bacteria. Created with BioRender.com. (Right panel) 1% gel electrophoresis of Site Directed Mutagenesis PCR products containing gRNA edits targeting *dop-1* and *dop-4*. First lane is pDD162 CRISPR Cas9 vector control. Second lane is plasmid built from vector by site directed mutagenesis containing gRNA sequence targeting

the *dop-1* locus. Third lane is plasmid containing gRNA sequence targeting the *dop-4* locus.

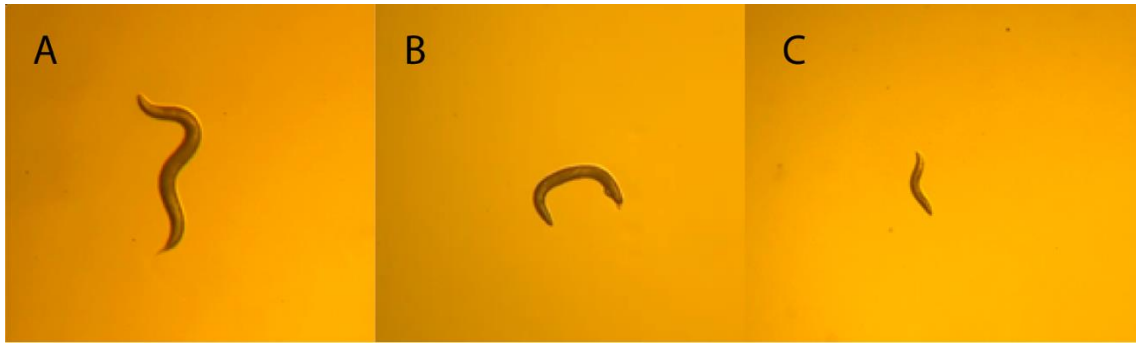


Figure 8. *C. elegans* phenotypes used for screening in Strategies 1 and 2. (A) N2 *C. elegans* phenotype. (B) Rol phenotype, in characteristic horseshoe shape. Rol phenotype is indicative of heterozygous (*dpy-10/+*) Co-CRISPR edits in Strategy 1. Rol phenotype is also indicative of *sqt-1* edits conferred by SEC in Strategy 2. (C) Dpy phenotype indicative of homozygous (*dpy-10/dpy-10*) Co-CRISPR edits in Strategy 1.

$$\begin{array}{l}
\mathbf{P:} \quad \text{♀} \frac{gfp::dop-1}{+}; \frac{mut}{+} \times N2 \quad \text{♂} \frac{+}{\emptyset}; \frac{+}{+} \\
\downarrow \\
\mathbf{F1:} \quad \text{♂} \frac{gfp::dop-1}{\emptyset}; \left[\frac{mut}{+} \text{ or } \frac{+}{+} \right] \times N2 \quad \text{♀} \frac{+}{+}; \frac{+}{+} \\
\downarrow \\
\mathbf{F2:} \quad \text{♂} \frac{gfp::dop-1}{\emptyset}; \left[\frac{mut}{+} \text{ or } \frac{+}{+} \right] \times N2 \quad \text{♀} \frac{+}{+}; \frac{+}{+}
\end{array}$$

Figure 9. Outcrossing strategy. Founder worms will be crossed with N2 males. F1 males confirmed for the edit, *gfp::dop-1* in this example, are crossed to N2 hermaphrodites. This cross is repeated for 4-6 generations.

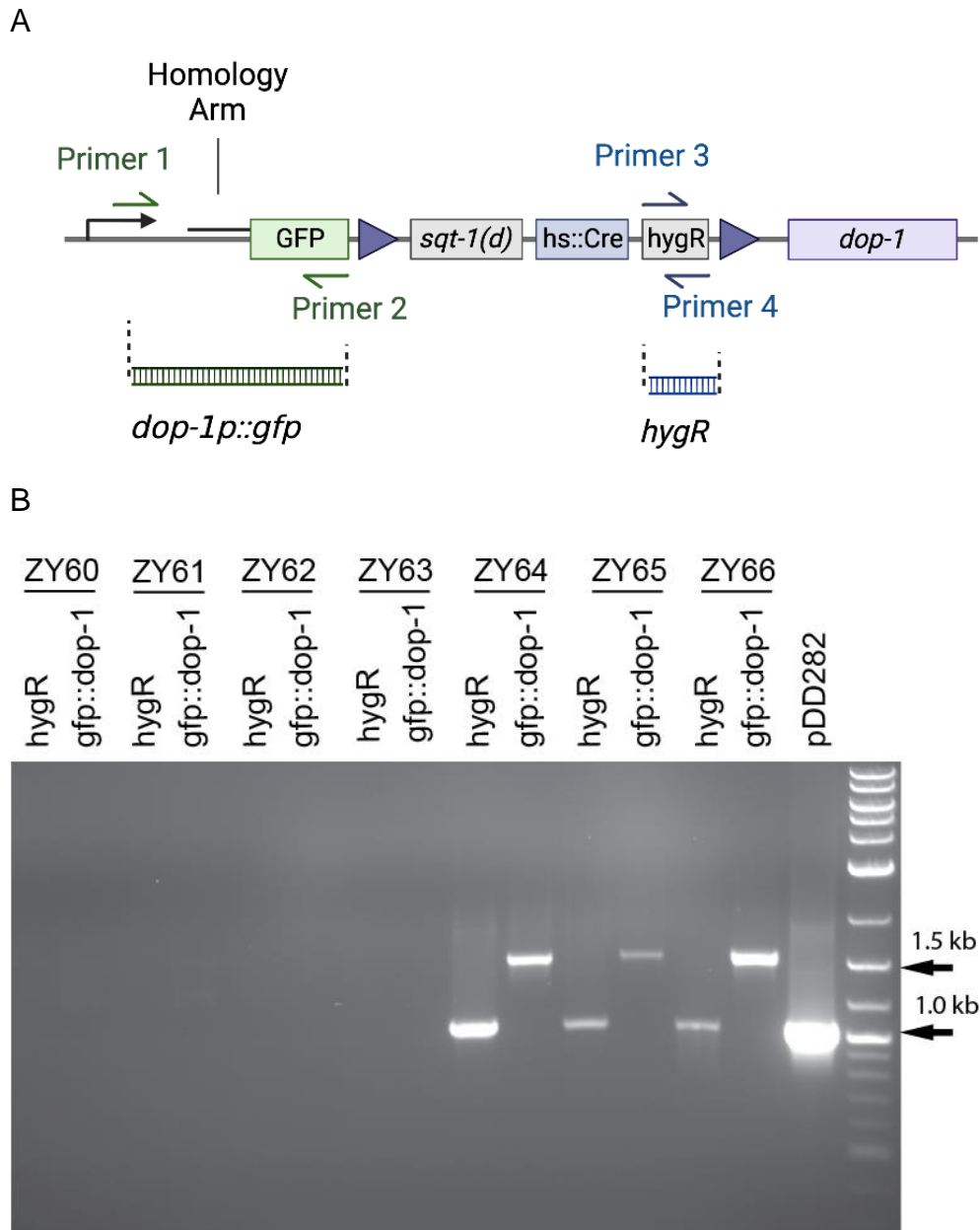


Figure 10. Three candidate *C. elegans* lines contained the hygromycin resistance gene and *gfp::dop-1* insert conferred by repair template plasmid. (A) Schematic of PCR primers used to interrogate genomic DNA for *dop-1::gfp* (using primers 1 and 2) and *hygR* (using primers 3 and 4). Primer 1 is upstream of *dop-1*

sequence used for 5' Homology Arm in repair template plasmid, indicating PCR product is generated from genomic edit and not repair template. Created with BioRender.com. (B) 1.5% gel electrophoresis of candidate lysates with primers interrogating for the hygromycin resistance gene and *gfp::dop-1* insert. Final lane is vector plasmid pDD282, from which the repair template was build and thus served as positive control for hygromycin resistance gene.

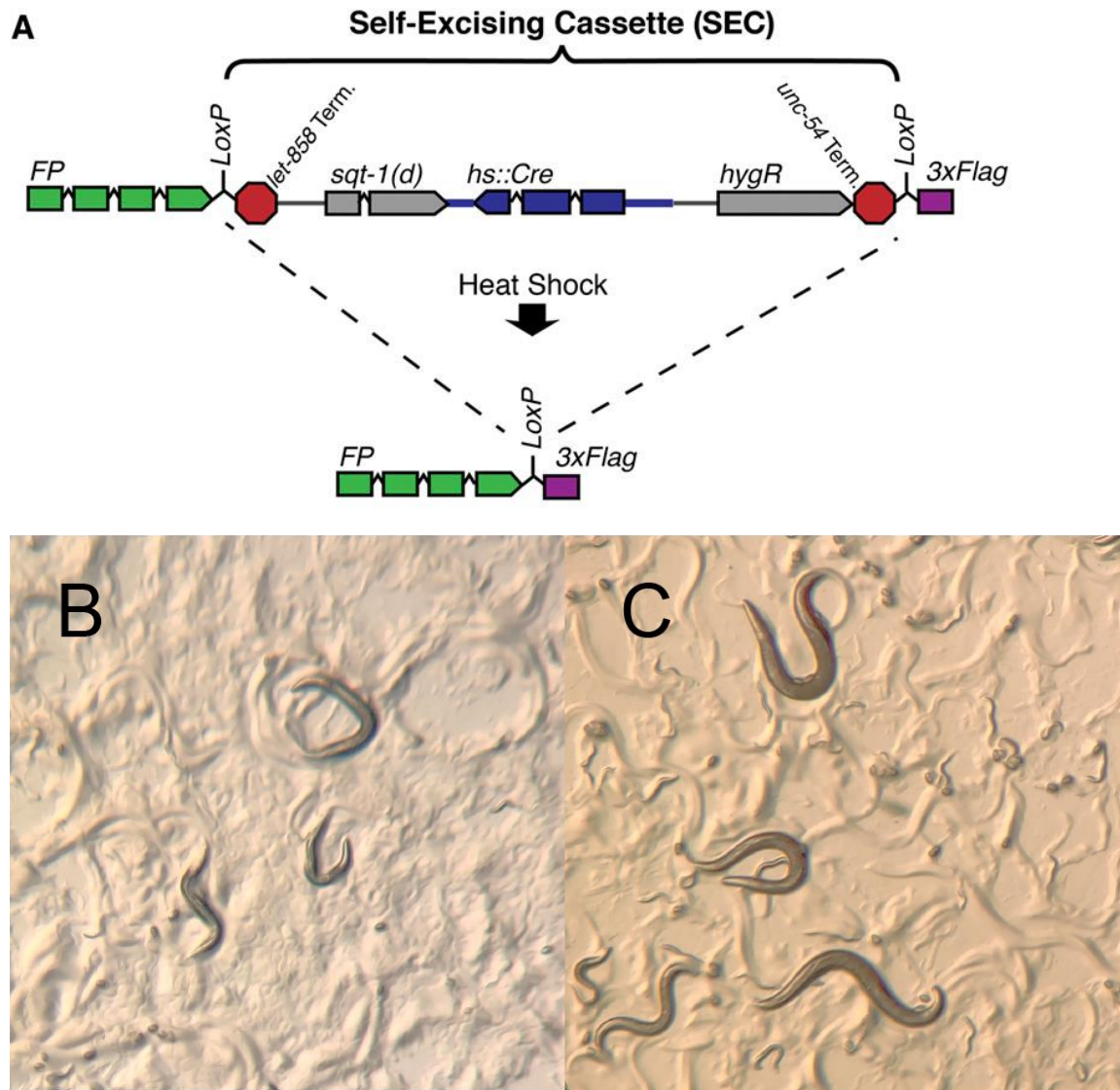


Figure 11. Strategy 2 selection strategy overview. (A) Repair template insert with contents of self-excising cassette (SEC), adapted from (Dickinson et al., 2015). Repair template contains a gene encoding a fluorescent protein followed by the SEC with flanking LoxP sites. SEC contains a gene encoding a dominant, mutant *sqt-1* allele, gene encoding Cre recombinase under control of a heat shock inducible promoter, and gene encoding hygromycin resistance. Following heat

shock, Cre recombinase removes SEC, leaving LoxP scar hidden in an intron. Panels B and C depict phenotypes of candidate strains before (B) and after (C) heat shock induced Cre-lox excision of SEC using Strategy 2. (B) Candidate worms exhibiting the characteristic Rol phenotype expressing the dominant, mutant *sqt-1* allele conferred by the SEC. These worms were also resistant to hygromycin selection (not shown). (C) Candidate worms exhibiting the wild type phenotype after heat shock induced removal of SEC containing mutant *sqt-1* allele. Following heat shock, these worms were now sensitive to hygromycin (not shown).

Dickinson, D. J., Pani, A. M., Heppert, J. K., Higgins, C. D., & Goldstein, B. (2015). Streamlined Genome Engineering with a Self-Excising Drug Selection Cassette. *Genetics*, 200(4), 1035–1049.
<https://doi.org/10.1534/genetics.115.178335>

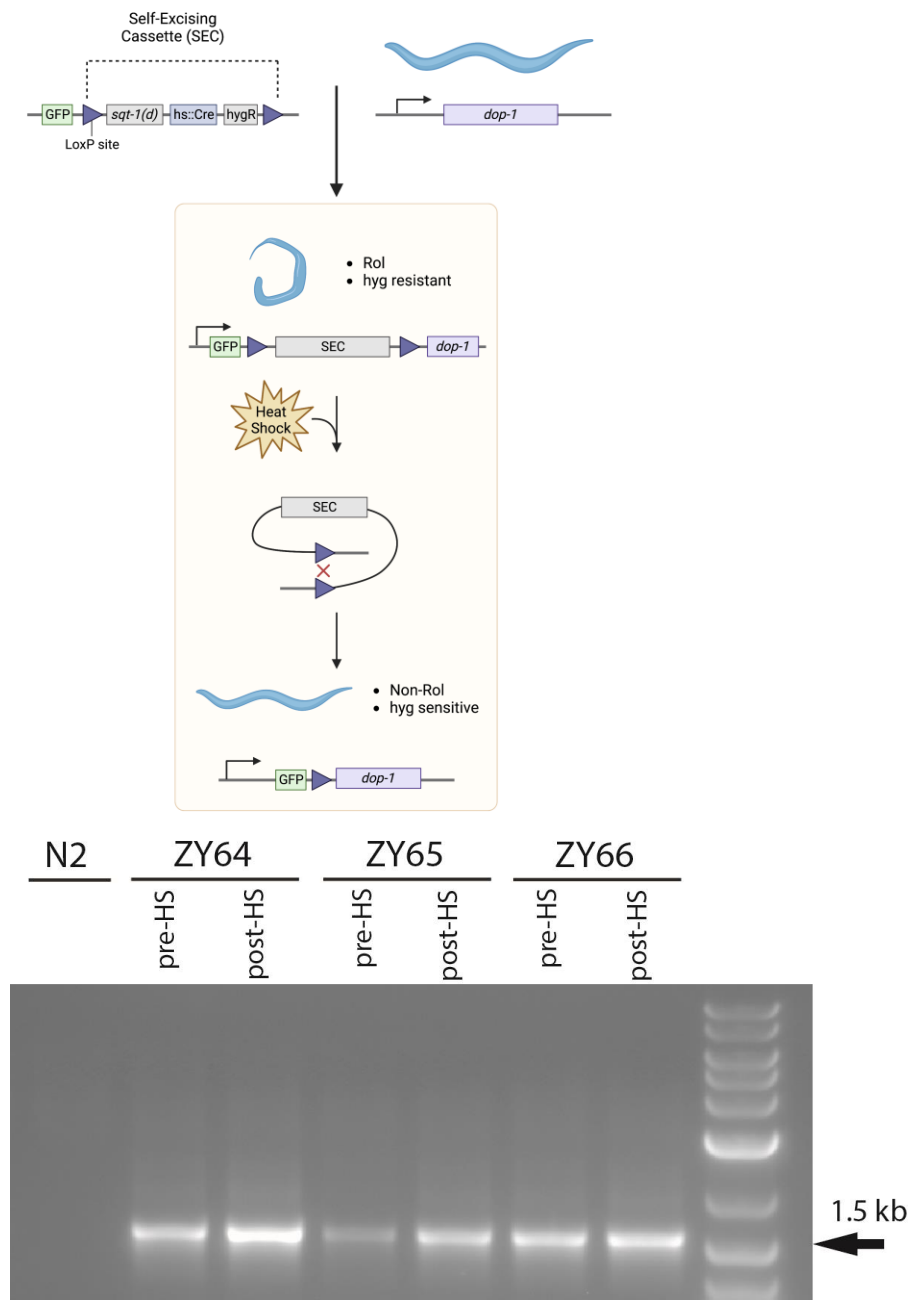


Figure 12. Candidate *C. elegans* lines ZY64, ZY65, and ZY66 maintained *gfp::dop-1* insert following heat shock induced SEC removal. 1% gel electrophoresis of *C. elegans* candidate lines with primers interrogating for *gfp::dop-1* insertion in both pre- and post-heat shock lysates. All three candidate

lines showed expected bands of about 1,600 bp before and after heat shock induced SEC removal.

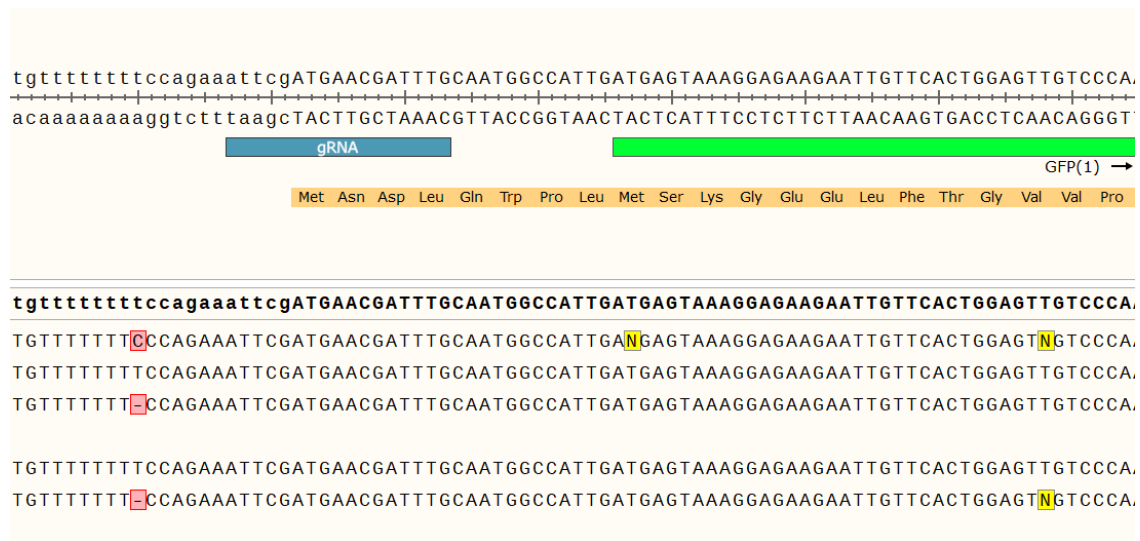


Figure 13. All 3 lines contained *gfp::dop-1* edit before and after heat shock. Alignment of sequences from *gfp::dop-1* PCR positive candidates ZY64, ZY65, and ZY66 both pre- and post-heat shock removal of SEC.

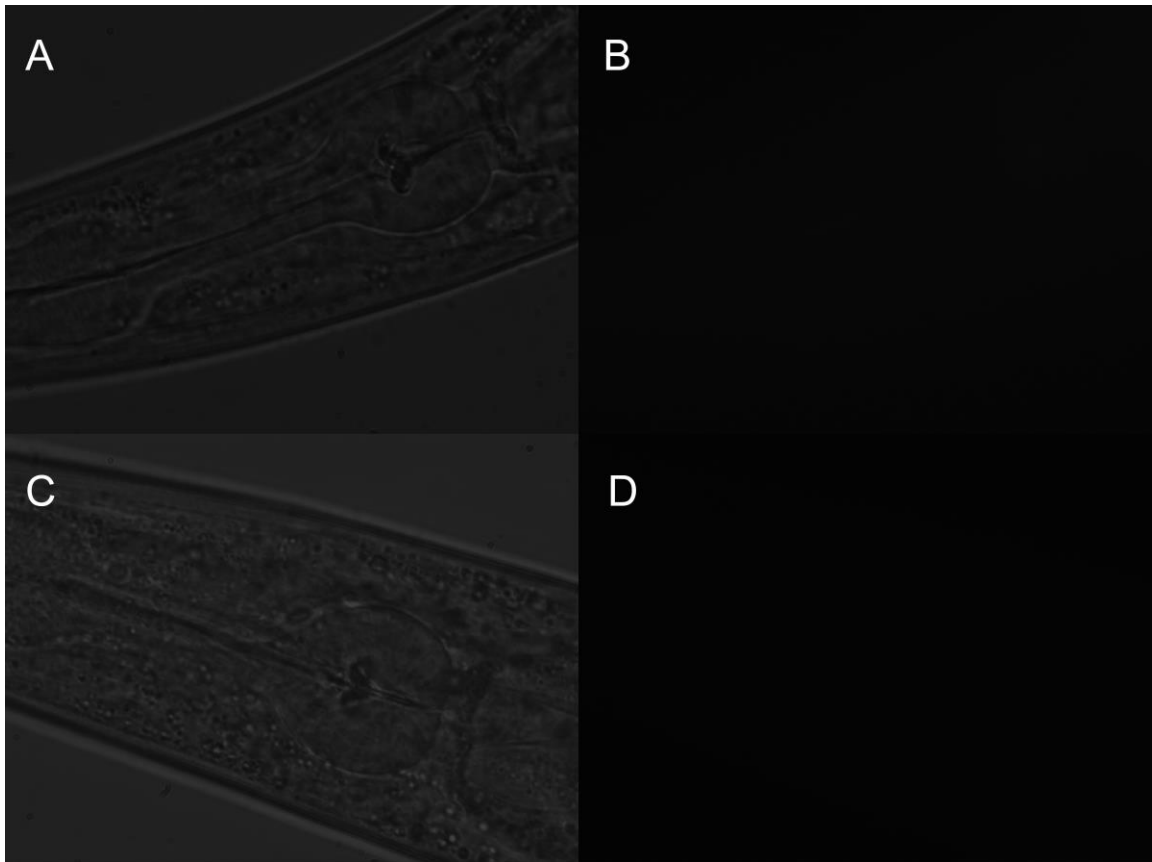


Figure 14. Edited *gfp::dop-1* worms did not exhibit detectable fluorescence. An N2 hermaphrodite head under brightfield (A) and UV fluorescence (B), and ZY65 hermaphrodite under brightfield (C) and UV fluorescence (D). Worms are representative of all 3 lines, before and after heat shock.

APPENDIX B:
TABLES

Table 1. List of Strategy 1 edits, repair templates and ssODNs used.

Edit	Size of PCR template	Primers used for PCR	Size bridge ssODN	Bridge ssODNs used
dop-1::mNeonGreen	915 bp	oZY63 & oZY64	66 nt & 66 nt	oZY69 & oZY70
dop-4::mNeonGreen	915 bp	oZY63 & oZY65	66 nt & 66 nt	oZY71 & oZY72
dop-1::mCherry:unc-54 3' UTR	1,658 bp	oZY65 & oZY66	66 nt & 66 nt	oZY73 & oZY74
dop-4::mCherry:unc-54 3' UTR	1,658 bp	oZY65 & oZY67	66 nt & 66 nt	oZY75 & oZY76

Table 2. Sequences of oligonucleotides used in Strategy 1.

PCR Primers			
Name	F/R	Description	Sequence (5' to 3')
oZY63	F	mNeonGreen amplification	ATGGTGTCTGAAGGGAGAAGAGG
oZY64	R	mNeonGreen amplification	CTACTTGTAGAGTTCATCCATTCCCATCAC
oZY65	F	mCherry + unc-54 3' UTR amplification	ATGGTCTCAAAGGGTGAAGAAG
oZY66	R	mCherry + unc-54 3' UTR amplification	AAACAGTTATGTTTGGTATATTGGG
ssODNs			
Name	S/AS	Description	Sequence (5' to 3')
oZY69	S	Bridging 5' end of dop-1 to mNG	aatgtttttttccagaaattcgATGAACGATTGATGGTGTCTGAAGGGAGAAGAGGATAACATGG
oZY70	AS	Bridging 3' end of dop-1 to mNG	CAAGACGGAGAATAATCCGAGCAATGGCCATTGCTACTTGTAGAGTTCATCCATTCCCATCACATC
oZY71	S	Bridging 5' end of dop-4 to mNG	catcaaaATGTTGGCTTACGGGTCTGATCCGAACATGGTGTCTGAAGGGAGAAGAGGATAACATGGC
oZY72	AS	Bridging 3' end of dop-4 to mNG	GGACGGTGTCTATTGTGATATAGAGGTCTTCGGCCTACTTGTAGAGTTCATCCATTCCCATCACATC
oZY73	S	Bridging 5' end of dop-1 to mCherry	tggtttttttccagaaattcgATGAACGATTGATGTCTCAAAGGGTGAAGAAGATAACATGGCA
oZY74	AS	Bridging 3' end of dop-1 to mCherry	CAAGACGGAGAATAATCCGAGCAATGGCCATTGaaacagttatgttttggtatattgggaatgtatt
oZY75	S	Bridging 5' end of dop-4 to mCherry	atcaaaATGTTGGCTTACGGGTCTGATCCGAACATGGTCTCAAAGGGTGAAGAAGATAACATGGCA
oZY76	AS	Bridging 3' end of dop-4 to mCherry	GGACGGTGTCTATTGTGATATAGAGGTCTTCGGCaaacagttatgttttggtatattgggaatgtatt

Primers used to PCR amplification of repair template and ssODNs used to facilitate HDR. Lowercase letters indicate bases in regulatory regions such as promoters or 3' UTRs. Capital letters indicate exon coding sequences. Letters in green indicate coding sequence for GFP. Letters in red indicate coding sequence for mCherry.

Table 3. List of primers used for plasmid editing of Strategy 2.

Primers			
Name	F/R	Description	Sequence (5' to 3')
oZY58	F	Insert dop-1 gRNA into Cas9 vector pDD162 (pZY22)	cgatttgcaaGTTTTAGAGCTAGAAATAG C
oZY59	R	Insert dop-1 gRNA into Cas9 vector pDD162 (pZY22)	ttcatcgaatCAAGACATCTCGCAATAG
oZY60	F	Insert dop-4 gRNA into Cas9 vector pDD162 (pZY23)	cttcggcggttGTTTTAGAGCTAGAAATAGC
oZY61	R	Insert dop-4 gRNA into Cas9 vector pDD162 (pZY23)	acctctatatCAAGACATCTCGCAATAG
oZY67	F	pZY22 & pZY23 Sequencing primers	GTTATGAAATGCCTACACCCTCTC
oZT68	R	pZY22 & pZY23 Sequencing primers	TGCGCAACTGTTGGGAAG
oZY77	F	Forward primer for insertion of 5' homology arm to <i>dop-1</i> into FP:SEC vector	acgttgtaaaacgacggccagtcgccggcaCTC TTGAATCCGCTTGATACTC
oZY78	R	Reverse primer for insertion of 5' homology arm to <i>dop-1</i> into FP:SEC vector	TCCAGTGAACAATTCTTCTCCTTTACTC ATCAATGGCCATTGCAAATCGTTC
oZY79	F	Forward primer for insertion of 3' homology arm to <i>dop-1</i> into FP:SEC vector	CGTGATTACAAGGATGACGATGACAA GAGACTCGGATTATTCTCCGTCTT
oZY80	R	Reverse primer for insertion of 3' homology arm to <i>dop-1</i> into FP:SEC vector	tcacacaggaaacagctatgaccatgttatcgagt cctccttgattttctac
oZY81	F	Forward primer for insertion of 5' homology arm to dop-4 into FP:SEC vector	acgttgtaaaacgacggccagtcgccggcaagtc ttagaagtgagctcagg

oZY82	R	Reverse primer for insertion of 5' homology arm to dop-4 into FP:SEC vector	TCCAGTGAACAATTCTTCTCCTTTACTC ATCGGCGTTCGGATCAGACC
oZY83	F	Forward primer for insertion of 3' homology arm to dop-4 into FP:SEC vector	CGTGATTACAAGGATGACGATGACAA GAGAAAGACCTCTATATCACAATG
oZY84	R	Reverse primer for insertion of 3' homology arm to dop-4 into FP:SEC vector	tcacacaggaaacagctatgaccatgttatggatc tctttccgtacaacttttcggg

Lowercase letters indicate bases in regulatory regions (such as promoters or 3' UTRs). Capital letters indicate exon coding sequences.

Table 4.

Gene	Expression Level (TPM)				
	ASH	AUA	AVA	AVB	AVD
<i>dop-1</i>	0	88.15	230.57	97.02	118.2
<i>dop-2</i>	257.73	0	249.62	0	0
<i>dop-3</i>	128.53	0	78.56	99.64	108.96
<i>dop-4</i>	0	0	45.47	82.16	0
<i>ser-4</i>	99.85	0	0	0	0
<i>ser-7</i>	0	294.50	0	0	0
<i>glr-1</i>	0	35.59	893.57	0	677.11
<i>glr-4</i>	0	44.16	183.54	85.84	173.77
<i>his-72</i>	230.29	477.79	608.28	337.81	424.81

Single cell RNA sequencing data showing expression of various genes in

Transcripts per Million (TPM). Dopamine receptors *dop-1* through *dop-4*.

Serotonin receptors *ser-4* and *ser-7*. Glutamate receptors *glr-1* and *glr-4*. Widely expressed Histone H3 *his-72*.

APPENDIX C:
LIST OF ABBREVIATIONS

List of Abbreviations

CRISPR - clustered regularly interspersed short palindromic repeats

DA – dopamine

Dpy – Dumpy phenotype

dsDNA - double stranded DNA

FP - fluorescent protein

HA - homology arms

HDR - homology directed repair

mNG - monomeric Neon Green

NHEJ - non-homologous end joining

PAM – protospacer adjacent motif

PCR - polymerase chain reaction

Rol – Roller phenotype

SEC – self-excising cassette

ssODN - single-stranded oligodeoxynucleotide

TALEN - transcription activator-like effector nuclease

ZFN - zinc finger nucleases

REFERENCES

- Arribere, J. A., Bell, R. T., Fu, B. X. H., Artilles, K. L., Hartman, P. S., & Fire, A. Z. (2014). Efficient Marker-Free Recovery of Custom Genetic Modifications with CRISPR/Cas9 in *Caenorhabditis elegans*. *Genetics*, 198(3), 837–846. <https://doi.org/10.1534/genetics.114.169730>
- Bargmann, C. I. (1998). Neurobiology of the *Caenorhabditis elegans* Genome. *Science*, 282(5396), 2028–2033. <https://doi.org/10.1126/science.282.5396.2028>
- Brockie, P. (2006). Ionotropic glutamate receptors: Genetics, behavior and electrophysiology. *WormBook*. <https://doi.org/10.1895/wormbook.1.61.1>
- Chase, D. L., Pepper, J. S., & Koelle, M. R. (2004). Mechanism of Extrasynaptic Dopamine Signaling in *Caenorhabditis Elegans*. *Nature Neuroscience*, 7(10), 1096–1103. <https://doi.org/10.1038/nn1316>
- Concordet, J.-P., & Haeussler, M. (2018). CRISPOR: Intuitive Guide Selection for CRISPR/Cas9 Genome Editing Experiments and Screens. *Nucleic Acids Research*, 46(W1), W242–W245. <https://doi.org/10.1093/nar/gky354>
- Cong, L., Ran, F. A., Cox, D., Lin, S., Barretto, R., Habib, N., Hsu, P. D., Wu, X., Jiang, W., Marraffini, L. A., & Zhang, F. (2013). Multiplex genome engineering using CRISPR/Cas systems. *Science (New York, N.Y.)*, 339(6121), 819–823. <https://doi.org/10.1126/science.1231143>
- Cousins, M. S., & Salamone, J. D. (1996). Involvement of Ventrolateral Striatal Dopamine in Movement Initiation and Execution: A Microdialysis and

- Behavioral Investigation. *Neuroscience*, 70(4), 849–859.
[https://doi.org/10.1016/0306-4522\(95\)00407-6](https://doi.org/10.1016/0306-4522(95)00407-6)
- Culotti, J. G., & Russell, R. L. (1978). Osmotic Avoidance Defective Mutants of the Nematode *Caenorhabditis elegans*. *Genetics*, 90(2), 243–256.
- Davis, M. W. (n.d.). *ApE- A plasmid Editor*. Retrieved May 26, 2020, from
<https://jorgensen.biology.utah.edu/wayned/ape/>
- Dickinson, D. J., Pani, A. M., Heppert, J. K., Higgins, C. D., & Goldstein, B. (2015). Streamlined Genome Engineering with a Self-Excising Drug Selection Cassette. *Genetics*, 200(4), 1035–1049.
<https://doi.org/10.1534/genetics.115.178335>
- Dokshin, G. A., Ghanta, K. S., Piscopo, K. M., & Mello, C. C. (2018). Robust Genome Editing with Short Single-Stranded and Long, Partially Single-Stranded DNA Donors in *Caenorhabditis elegans*. *Genetics*, 210(3), 781–787. <https://doi.org/10.1534/genetics.118.301532>
- Durbin, R. M. (1987). *Studies on the development and organisation of the nervous system of Caenorhabditis elegans*. University of Cambridge.
- Evans, T. C. (2006). Transformation and Microinjection. *WormBook*, 10.
- Ezcurra, M., Tanizawa, Y., Swoboda, P., & Schafer, W. R. (2011). Food Sensitizes *C. elegans* Avoidance Behaviours Through Acute Dopamine Signalling. *The EMBO Journal*, 30(6), 1110–1122.
<https://doi.org/10.1038/emboj.2011.22>

- Ezcurra, M., Walker, D. S., Beets, I., Swoboda, P., & Schafer, W. R. (2016). Neuropeptidergic Signaling and Active Feeding State Inhibit Nociception in *Caenorhabditis elegans*. *Journal of Neuroscience*, 36(11), 3157–3169.
<https://doi.org/10.1523/JNEUROSCI.1128-15.2016>
- Faumont, S., & Lockery, S. R. (2006). The Awake Behaving Worm: Simultaneous Imaging of Neuronal Activity and Behavior in Intact Animals at Millimeter Scale. *Journal of Neurophysiology*, 95(3), 1976–1981.
<https://doi.org/10.1152/jn.01050.2005>
- Fay, D. S. (2013). Classical Genetic Methods. *WormBook*, 1–58.
<https://doi.org/10.1895/wormbook.1.165.1>
- Frøkjaer-Jensen, C., Davis, M. W., Hopkins, C. E., Newman, B. J., Thummel, J. M., Olesen, S.-P., Grunnet, M., & Jorgensen, E. M. (2008). Single-Copy Insertion of Transgenes in *Caenorhabditis elegans*. *Nature Genetics*, 40(11), 1375–1383. <https://doi.org/10.1038/ng.248>
- Gerfen, C. R. (1992). The Neostriatal Mosaic: Multiple Levels of Compartmental Organization in the Basal Ganglia. *Annual Review of Neuroscience*, 15, 285–320.
- Gerstein, M. B., Lu, Z. J., Van Nostrand, E. L., Cheng, C., Arshinoff, B. I., Liu, T., Yip, K. Y., Robilotto, R., Rechtsteiner, A., Ikegami, K., Alves, P., Chateigner, A., Perry, M., Morris, M., Auerbach, R. K., Feng, X., Leng, J., Vielle, A., Niu, W., ... Waterston, R. H. (2010). Integrative analysis of the *Caenorhabditis elegans* genome by the modENCODE project. *Science*

(New York, N.Y.), 330(6012), 1775–1787.

<https://doi.org/10.1126/science.1196914>

Ghanta, K. S., & Mello, C. C. (2020). Melting dsDNA Donor Molecules Greatly Improves Precision Genome Editing in *Caenorhabditis elegans*. *Genetics*, 216(3), 643–650. <https://doi.org/10.1534/genetics.120.303564>

Hammarlund, M., Hobert, O., Miller, D. M., & Sestan, N. (2018). The CeNGEN Project: The Complete Gene Expression Map of an Entire Nervous System. *Neuron*, 99(3), 430–433.

<https://doi.org/10.1016/j.neuron.2018.07.042>

Hilliard, M. A., Bargmann, C. I., & Bazzicalupo, P. (2002). *C. elegans* Responds to Chemical Repellents by Integrating Sensory Inputs from the Head and the Tail. *Current Biology*, 12(9), 730–734. [https://doi.org/10.1016/S0960-9822\(02\)00813-8](https://doi.org/10.1016/S0960-9822(02)00813-8)

Hilliard, M. A., Bergamasco, C., Arbucci, S., Plasterk, R. H., & Bazzicalupo, P. (2004). Worms Taste Bitter: ASH Neurons, QUI-1, GPA-3 and ODR-3 Mediate Quinine Avoidance in *Caenorhabditis elegans*. *The EMBO Journal*, 23(5), 1101–1111. <https://doi.org/10.1038/sj.emboj.7600107>

Jansen, R., Embden, J. D. A. van, Gastra, W., & Schouls, L. M. (2002). Identification of genes that are associated with DNA repeats in prokaryotes. *Molecular Microbiology*, 43(6), 1565–1575. <https://doi.org/10.1046/j.1365-2958.2002.02839.x>

- Jinek, M., Chylinski, K., Fonfara, I., Hauer, M., Doudna, J. A., & Charpentier, E. (2012). A Programmable Dual-RNA–Guided DNA Endonuclease in Adaptive Bacterial Immunity. *Science*, 337(6096), 816–821.
<https://doi.org/10.1126/science.1225829>
- Kaplan, J. M., & Horvitz, H. R. (1993). A Dual Mechanosensory and Chemosensory Neuron in *Caenorhabditis elegans*. *Proceedings of the National Academy of Sciences*, 90(6), 2227–2231.
<https://doi.org/10.1073/pnas.90.6.2227>
- Knable, M. B., & Weinberger, D. R. (1997). Dopamine, the Prefrontal Cortex and Schizophrenia. *Journal of Psychopharmacology*, 11(2), 123–131.
<https://doi.org/10.1177/026988119701100205>
- Koob, G. F. (1992). Drugs of Abuse: Anatomy, Pharmacology and Function of Reward Pathways. *Trends in Pharmacological Sciences*, 13(5), 177–184.
- Koob, G. F., & Bloom, F. E. (1988). Cellular and Molecular Mechanisms of Drug Dependence. *Science*, 242(4879), 715–724.
- Lang AE & Lozano AM. (1998). Medical Progress. Parkinson's Disease: First of Two Parts. *New England Journal of Medicine*, 339(15), 1044–1054.
- Le Moal, M., & Simon, H. (1991). Mesocorticolimbic Dopaminergic Network: Functional and Regulatory Roles. *Physiological Reviews*, 71(1), 155–234.
<https://doi.org/10.1152/physrev.1991.71.1.155>
- Lints, R., & Emmons, S. W. (1999). *Dopaminergic Neurons in C. elegans*. 13.

- Madhu, B., Lakdawala, M. F., & Gumienny, T. L. (2022). Small-scale Extraction of *Caenorhabditis elegans* Genomic DNA. *Journal of Visualized Experiments*, 184, 63716. <https://doi.org/10.3791/63716>
- Mango, S. E. (2001). Stop making nonSense: The *C. elegans smg* genes. *Trends in Genetics*, 17(11), 646–653. [https://doi.org/10.1016/S0168-9525\(01\)02479-9](https://doi.org/10.1016/S0168-9525(01)02479-9)
- Mello, C. C., Kramer, J. M., Stinchcomb, D., & Ambros, V. (1991). Efficient Gene Transfer in *C. elegans*: Extrachromosomal Maintenance and Integration of Transforming Sequences. *The EMBO Journal*, 10(12), 3959–3970.
- Missale, C., Nash, S. R., Robinson, S. W., Jaber, M., & Caron, M. G. (1998). Dopamine Receptors: From Structure to Function. *Physiological Reviews*, 78(1), 189–225. <https://doi.org/10.1152/physrev.1998.78.1.189>
- Mojica, F. J. M., Díez-Villaseñor, C., García-Martínez, J., & Soria, E. (2005). Intervening Sequences of Regularly Spaced Prokaryotic Repeats Derive from Foreign Genetic Elements. *Journal of Molecular Evolution*, 60(2), 174–182. <https://doi.org/10.1007/s00239-004-0046-3>
- Mojica, F. J. M., Ferrer, C., Juez, G., & Rodríguez-Valera, F. (1995). Long stretches of short tandem repeats are present in the largest replicons of the Archaea *Haloferax mediterranei* and *Haloferax volcanii* and could be involved in replicon partitioning. *Molecular Microbiology*, 17(1), 85–93. https://doi.org/10.1111/j.1365-2958.1995.mmi_17010085.x

- Paix, A., Folkmann, A., Rasoloson, D., & Seydoux, G. (2015). High Efficiency, Homology-Directed Genome Editing in *Caenorhabditis elegans* Using CRISPR-Cas9 Ribonucleoprotein Complexes. *Genetics*, 201(1), 47–54.
<https://doi.org/10.1534/genetics.115.179382>
- Pourcel, C., Salvignol, G., & Vergnaud, G. (2005). CRISPR elements in *Yersinia pestis* acquire new repeats by preferential uptake of bacteriophage DNA, and provide additional tools for evolutionary studies. *Microbiology (Reading, England)*, 151(Pt 3), 653–663.
<https://doi.org/10.1099/mic.0.27437-0>
- Prior, H., Jawad, A. K., MacConnachie, L., & Beg, A. A. (2017). Highly Efficient, Rapid and Co-CRISPR-Independent Genome Editing in *Caenorhabditis elegans*. *G3 Genes/Genomes/Genetics*, 7(11), 3693–3698.
<https://doi.org/10.1534/g3.117.300216>
- Robert, V., & Bessereau, J.-L. (2007). Targeted Engineering of the *Caenorhabditis elegans* Genome Following Mos1-Triggered Chromosomal Breaks. *The EMBO Journal*, 26(1), 170–183.
<https://doi.org/10.1038/sj.emboj.7601463>
- Saiardi, A., Bozzi, Y., Baik, J.-H., & Borrelli, E. (1997). Antiproliferative Role of Dopamine: Loss of D2 Receptors Causes Hormonal Dysfunction and Pituitary Hyperplasia. *Neuron*, 19(1), 115–126.
[https://doi.org/10.1016/S0896-6273\(00\)80352-9](https://doi.org/10.1016/S0896-6273(00)80352-9)

- Sambongi, Y., Nagae, T., Liu, Y., Yoshimizu, T., Takeda, K., Wada, Y., & Futai, M. (1999). Sensing of Cadmium and Copper Ions by Externally Exposed ADL, ASE, and ASH Neurons Elicits Avoidance Response in *Caenorhabditis elegans*. *NeuroReport*, 10(4), 753.
- Sanyal, S., Wintle, R. F., Kindt, K. S., Nuttley, W. M., Arvan, R., Fitzmaurice, P., Bigras, E., Merz, D. C., Hebert, T. E., van der Kooy, D., Schafer, W. R., Culotti, J. G., & Van Tol, H. H. M. (2004). Dopamine Modulates the Plasticity of Mechanosensory Responses in *Caenorhabditis elegans*. *EMBO (European Molecular Biology Organization) Journal*, 23(2), 473–482. <https://doi.org/10.1038/sj.emboj.7600057>
- Schwartz, M. L., Davis, M. W., Rich, M. S., & Jorgensen, E. M. (2021). High-efficiency CRISPR gene editing in *C. elegans* using Cas9 integrated into the genome. *PLOS Genetics*, 17(11), e1009755. <https://doi.org/10.1371/journal.pgen.1009755>
- Stiernagle, T. (2006). Maintenance of *C. elegans*. *WormBook*. <https://doi.org/10.1895/wormbook.1.101.1>
- Sugiura, M., Fuke, S., Suo, S., Sasagawa, N., Van Tol, H. H. M., & Ishiura, S. (2005). Characterization of a novel D2-like dopamine receptor with a truncated splice variant and a D1-like dopamine receptor unique to invertebrates from *Caenorhabditis elegans*. *Journal of Neurochemistry*, 94(4), 1146–1157. <https://doi.org/10.1111/j.1471-4159.2005.03268.x>

- Sulston, J., Dew, M., & Brenner, S. (1975). Dopaminergic Neurons in the Nematode *Caenorhabditis elegans*. *Journal of Comparative Neurology*, 163(2), 215–226. <https://doi.org/10.1002/cne.901630207>
- Suo, S., Sasagawa, N., & Ishiura, S. (2002). Identification of a Dopamine Receptor from *Caenorhabditis elegans*. *Neuroscience Letters*, 319(1), 13–16. [https://doi.org/10.1016/S0304-3940\(01\)02477-6](https://doi.org/10.1016/S0304-3940(01)02477-6)
- Suo, S., Sasagawa, N., & Ishiura, S. (2003). Cloning and Characterization of a *Caenorhabditis elegans* D2-Like Dopamine Receptor. *Journal of Neurochemistry*, 86(4), 869–878. <https://doi.org/10.1046/j.1471-4159.2003.01896.x>
- Tsalik, E. L., Niacaris, T., Wenick, A. S., Pau, K., Avery, L., & Hobert, O. (2003). LIM Homeobox Gene-Dependent Expression of Biogenic Amine Receptors in Restricted Regions of the *C. elegans* Nervous System. *Developmental Biology*, 263(1), 81–102. [https://doi.org/10.1016/S0012-1606\(03\)00447-0](https://doi.org/10.1016/S0012-1606(03)00447-0)
- Varshney, L. R., Chen, B. L., Paniagua, E., Hall, D. H., & Chklovskii, D. B. (2011). Structural Properties of the *Caenorhabditis elegans* Neuronal Network. *PLOS Computational Biology*, 7(2), e1001066. <https://doi.org/10.1371/journal.pcbi.1001066>
- Vicencio, J., Martínez-Fernández, C., Serrat, X., & Cerón, J. (2019). Efficient Generation of Endogenous Fluorescent Reporters by Nested CRISPR in

Caenorhabditis elegans. *Genetics*, 211(4), 1143–1154.

<https://doi.org/10.1534/genetics.119.301965>

Vidal-Gadea, A. G., & Pierce-Shimomura, J. T. (2012). Conserved Role of Dopamine in the Modulation of Behavior. *Communicative & Integrative Biology*, 5(5), 440–447. <https://doi.org/10.4161/cib.20978>

White, J. G., Southgate, E., Thomson, J. N., & Brenner, S. (1986). The Structure of the Nervous System of the Nematode *Caenorhabditis elegans*. *Philos Trans R Soc Lond B Biol Sci*, 314(1165), 1–340.

Zengcai V Guo, Anne C Hart, & Sharad Ramanathan. (2009). Optical Interrogation of Neural Circuits in *Caenorhabditis elegans*. *Nature Methods*, 6(12), 891–896. <https://doi.org/10.1038/nmeth.1397>